Friction
https://doi.org/10.1007/s40544-023-0833-0
ISSN 2223-7690
CN 10-1237/TH
REVIEW ARTICLE

Mechanism and application of mechanical property improvements in engineering materials by pulsed magnetic treatment: A review

Zhipeng CAI[1,2,3,*], Chengkai QIAN[2], Xu ZHANG[2], Ning DAI[2], Yao WU[3], Wen JI[3]

[1] *State Key Laboratory of Tribology in Advanced Equipment, Tsinghua University, Beijing 100084, China*

[2] *Department of Mechanical Engineering, Tsinghua University, Beijing 100084, China*

[3] *Tianjin Research Institute for Advanced Equipment, Tsinghua University, Tianjin 300304, China*

Received: 17 March 2023 / Revised: 24 July 2023 / Accepted: 21 September 2023

Abstract: Pulsed magnetic treatment (PMT) has been adopted as an effective strengthening method for engineering materials and components in recent years, and the development of its application depends on the comprehensive understanding of the nature of PMT. The deep mechanism was thought initially to be the magnetostrictive effect, while further investigation found that the magnetic field could lead to the change of the defect states in the crystal, which is called the magnetoplastic effect. Due to the complexity of the engineering materials, manifestations of the magnetoplastic effect become more diverse, and they were reviewed in the form of microstructure homogenization and interfacial stabilization. Further, the mechanism of the magnetoplastic effect was discussed, focusing on the changes in the spin states under the external magnetic field. Microstructure modifications could also alter material performances, especially the residual stress, plasticity, and fatigue properties. Therefore, PMT with specific parameters can be utilized to obtain an ideal combination of microstructure, residual stress, and mechanical properties for better service performance of different mechanical parts, and its applications on machining tools and bearings are perfect examples. This work reviews the effect of PMT on the microstructure and properties of different materials and the mechanism, and it also summarizes the fundamental applications of PMT on essential mechanical parts.

Keywords: pulsed magnetic treatment; wear resistance; microstructure modifications; mechanical properties; magnetoplastic effect

1 Introduction

The microstructure and properties of materials will change under the effect of different forms of external magnetic fields. The discovery has attracted many materials scientists and engineers to explore its applications and underlying mechanisms. One typical application is introducing the rotating magnetic field in the liquid metal pool during forging and welding [1, 2]. It can promote the transformation of coarse grains and dendrites into equiaxed grains by increasing heterogeneous nuclei in the molten metal and decreasing the temperature gradient ahead of the solid–liquid interface. As a result, the microstructure of the ingot and weld joint is refined, and the strength and ductility are improved. The magnetic field can also be coupled with heat treatments for phase transformation, including austenite [3, 4], martensite [5], and bainite [6] transformation. In addition, it can also reduce the retained austenite content and increase the carbide content during tempering [4]. Based on the theoretical calculation results, the magnetic field brings about the free energy of magnetization, increasing the stability of the ferrite.

* Corresponding author: Zhipeng CAI, E-mail: czpdme@mail.tsinghua.edu.cn

It is not hard to notice that the above magnetic field applications are realized at high temperatures. Naturally, it has also sparked researchers' curiosity on another issue: whether the microstructure and properties of materials may be affected by the magnetic field at room temperature. Attempts have already been made to apply the magnetic field on engineering materials and even specific workpieces at room temperature to improve their lifetime and reliability [7], and they have been converted to practical applications, the so-called pulsed magnetic treatment (PMT).

The application of PMT is achieved simply by mounting the pending workpiece in the pulsed magnetic field with specific parameters. Principal advantages that PMT offers in contrast to heat treatment are that it has a tiny thermal effect on the components, and the dimensions and appearances can be maintained. In addition, it is efficient to implement since there is no need of heating. Therefore, it is especially suitable as a final treatment for precision parts. The first magnetic treatment equipment designed for machining tools, called FluxaTron U102, was set up by INNOVEX (US), which can improve the performance of high-speed steel and cemented carbide tools in only 42 s. The service life of tools can be generally improved by 20%–50% and even more incredible than 150% in some specific applications [8, 9]. Later, along with applied researches, specific apparatus aimed at high-end components in aviation, automobile, engineering machinery, etc., have also been successfully fabricated by steps [10]. At present, there is a growing trend that the applications of PMT are migrated to a broader range of engineering parts such as bearings, dampers, and bolts [11].

Despite the smooth and successful application of PMT, its underlying mechanism remains unclear. The effect of the magnetic field on materials at room temperature may be traced back to James Joule who observed the dimension change of an iron sample during its magnetization process, which is the so-called magnetostriction effect. Experiments indicate that the magnetostriction effect is restricted to ferromagnetic materials. Surprisingly, in 1965, Zagoruiko [12] found that the external pulsed magnetic field could promote the dislocation mobility in paramagnetic NaCl crystals. This author attributed the motion of charged dislocations to the vortex electric fields produced by magnetic field variation. The same year, Chebotkevich et al. [13] reported the phenomenon of dislocation motion in Fe crystal by applying the magnetic field repeatedly. Later, Hayashi et al. [14] found that the alternating magnetic field applied along the tensile direction can reduce the flow stress in the monocrystalline Ni stretched at approximate liquid-nitrogen temperature. The latter two phenomena were interpreted as a result of the magnetostriction effect induced by the magnetic field as ferromagnetic materials were used in the research.

With a growing number of reports on magnetic induced microstructure modifications, some scholars have proposed different views. Alshits et al. [15] further studied the dislocation mobility in NaCl crystals under the magnetic field. It was found that the dislocations moved a distance without any external mechanical load after exposure. Alshits first named such a phenomenon as the magnetoplastic effect. Since then, most researchers have retained the usage of this term to describe similar phenomena of defect motion. For a long time afterwards, researches were mainly focused on simple material systems such as alkali halide crystals including NaCl, LiF, CsI, etc. [16–19], metals including monocrystalline Zn and Al [20–24] and semi-conductors including InSb and GaAs [25–27] were conducted. It has been proven that defect motion is a common phenomenon under the magnetic field.

However, the effect of PMT on the microstructure becomes much more sophisticated when scaled to the engineering materials. It is because there are different kinds of defects in engineering materials and their interaction cannot be overlooked. Without a clear view of the relationship between the magnetic field and the microstructure and mechanical property changes, promoting the PMT to the precision parts with complex and extreme service conditions has become the bottleneck of the PMT applications that has to be broken through. Therefore, there exists a large gap to narrow between researches of the magnetoplastic effect and the improvement in the mechanical properties of engineering materials, and it relies on insights into the deep mechanism of PMT.

The primary purpose of this paper is to review our

research on the effect of the pulsed magnetic field on the microstructure and mechanical properties of engineering materials at room temperature. Here, defect-related microstructure changes induced by PMT in engineering materials were introduced, and the underlying mechanism was further discussed based on the observations. Microstructure modifications induced by PMT also lead to mechanical property enhancement in the materials, and it has been applied to improve the service performance, especially the machining tools and bearings. It is expected to provide a reference for further understanding of the effect and the extended applications of PMT.

2 Effect of PMT on the microstructure and its mechanism

2.1 Microstructure modifications induced by PMT

PMT can cause atoms to permanently leave their initial positions and migrate to adjacent sites. Atomic migrations in crystalline materials are mainly achieved by vacancy diffusion and interstitial diffusion, and they are closely related to the defects. Therefore, changes in different types of defects are the major manifestation of the microstructure modifications induced by PMT. Here, observations of the point defect (vacancy) and line defect (dislocation) changes and their interactions in crystals were demonstrated respectively.

2.1.1 Effect of PMT on single defect

Point defect engineering is crucial for the performance of semiconductors, and the effect of the magnetic field on point defects in semiconductor materials has been widely researched. In order to increase the point defect density, monocrystalline Si doped with phosphorous by ion implantation was used [28]. Nano-indentation tests indicate that PMT can enhance the nano-hardness of the monocrystalline silicon. However, the strengthening effect can be reversed by subjecting the silicon sample to annealing at 800 °C for 780 s. Besides, the nano-hardness of the annealed monocrystalline silicon remains unchanged after PMT. It is inferred that PMT can promote the disbanding of vacancy clusters in the monocrystalline silicon to produce a large number of nonequilibrium vacancies, which can be attracted to adjacent dislocations and enhance the pinning effect. For validation of the theory, *in-situ* electron backscatter diffraction (EBSD) tests were performed on the silicon sample before and after PMT. The image quality (IQ) value obtained from the EBSD results is often used to characterize the local lattice distortion [29], and a higher IQ value represents a slighter lattice distortion. In contrast to the control sample, the IQ value increased apparently after PMT, indicating that the relaxation of the lattice distortion in the implantation layers occurred, and it must be accompanied by the state changes of the point defects.

Dislocation motion induced by PMT was commonly observed in crystalline materials. Alshits et al. [15] studied the dislocation mobility in NaCl crystals subjected to the magnetic field. Dislocations were introduced into the NaCl crystals by scratches, and they were revealed by chemical etching. As shown in Fig. 1(a), the dislocations moved tens to hundreds of micrometers after the NaCl crystals were exposed to a static magnetic field with a magnetic induction of approximately 0.5 T for several minutes, and no external mechanical load was applied. In the following years, a series of relevant research was conducted in other alkali halide crystals and metals [30–33]. A universal law is that the dislocations in the above materials can move under the external magnetic field, and the average distance of dislocation motion increases roughly linearly with the time of exposure to the magnetic field.

Golovin and Morgunov further studied relationship between the direction of the magnetic field and dislocation motion in the NaCl crystal exposed to the magnetic field [34]. They found that the numbers of dislocations moving along the [110], [$\bar{1}$10], [1$\bar{1}$0], and [$\bar{1}\bar{1}$0] directions of the NaCl crystal under a magnetic field of B=7 T were virtually identical. Besides, the slip distance of the dislocations is significantly higher than that in the control group, and the dislocation motion observed in the control group mainly originated from the error of etching, as shown in Figs. 1(b) and 1(c). They then concluded that the effect of the magnetic field on the dislocation motion is independent of the direction of the external magnetic field.

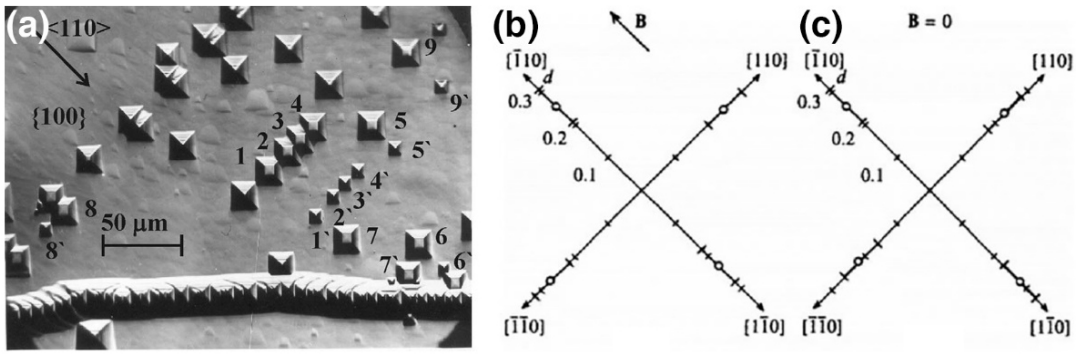

Fig. 1 Observations of the magnetoplastic effect: (a) etch patterns representing dislocation motion in the NaCl crystals: (1–9) initial dislocation positions and (1'–9') dislocation positions after exposure to a static magnetic field of 0.5 T for 2 min; fraction of dislocations *d* shifted in the four possible directions in the NaCl crystal, where the location of circle represents the average value of *d*, and the solid lines represent the upper and lower bounds of *d*: (b) crystals treated with a magnetic field pulse and (c) untreated crystal. Reproduced with permission from Ref. [8] for (a), © Elsevier Ltd. 2008; Ref. [34] for (b, c), © Springer Nature 1999.

2.1.2 *Comprehensive effect of PMT on microstructure*

Early studies mainly focused on point defects and dislocations solely, while their distribution and interaction were ignored. With the development in detection technology, more different phenomena have been reported, especially in engineering materials. Generally, they can be divided into two categories: homogenization of defect distributions and stabilization of surface defects.

The effect of PMT on steel was most frequently studied concerning ferromagnetic materials. Various analytical techniques have been applied to characterize the defect distribution in the sample. It was found with the transmission electron microscope (TEM) that dislocation cell walls in the 30CrMnSiA steel disappeared, and the dislocation distribution became uniform after magnetic treatment [35], as shown in Fig. 2. The effect of low-frequency PMT on the dislocation distribution of GCr15 bearing steel was also revealed [36]. TEM observations of the PMTed and the untreated samples showed that the dislocations in the untreated samples were concentrated in some regions, while those in the PMTed samples distributed more uniformly. It was believed in the beginning that the alternating magnetic field provides a driving force for dislocation depinning and slip through the alternating magnetostriction effect, i.e., the dimensions of the ferromagnetic materials change during the magnetization process [35]. However, the extent of the magnetostriction effect in the paramagnetic effect has been measured in the 45# steel subjected to PMT with different maximum currents, as shown in Fig. 3. Results have shown that the maximum is less than 15×10^6 with a maximum current of 120 A (which can generate a magnetic pulse with an amplitude of approximately 1.8 T), and it corresponds to the stress of 3.15 MPa [37], which is far lower than the required

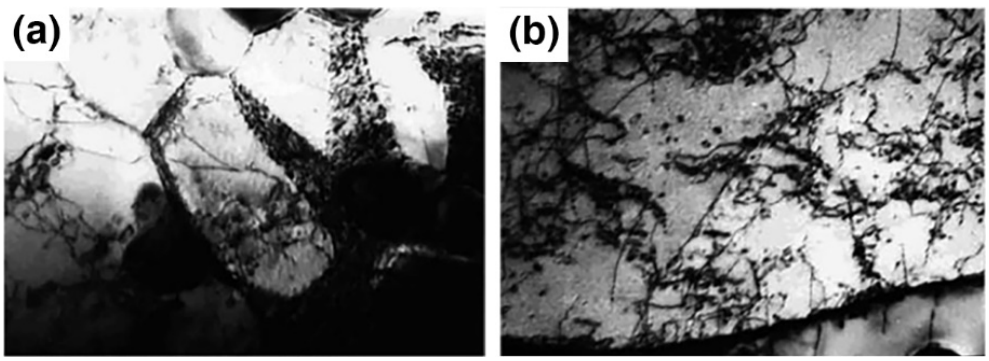

Fig. 2 TEM images revealing the dislocation distribution of 30CrMnSiA steel: (a) before magnetic treatment; (b) after magnetic treatment. Reproduced with permission from Ref. [35], © Elsevier Ltd. 2002.

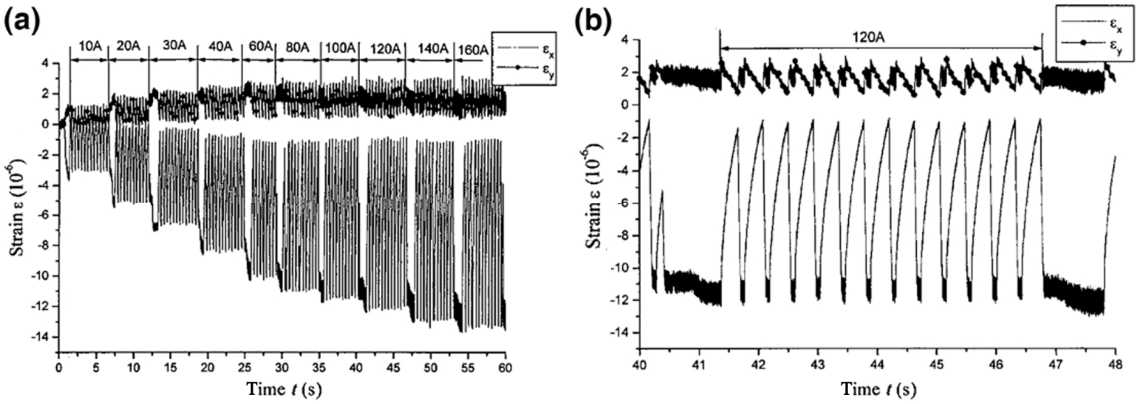

Fig. 3 (a) Magnetostriction curves recorded under different maximum currents; (b) magnified curve corresponding to 120 A. Reproduced with permission from Ref. [37], © SAGE Publications, Ltd. 2004.

driving force of approximately 40 MPa for dislocation motion based on the Peirls–Nabarro model [38]. Later, Huang [36] also reported that the magnetostriction of GCr15 steel during PMT was less than 10 με. Therefore, the magnetoplastic effect should play a key role in the process of PMT in addition to the magnetostriction effect.

With the growing attention, the effect of PMT on non-ferromagnetic engineering materials has been reported more frequently in recent years. The dislocation pile-up in 2014-T6 alloy is found to be relieved after the low-frequency alternating magnetic treatment [39]. As a result, the dislocation distributes more homogeneously among the grain. Regarding the Ti-6Al-4V titanium alloy, the variation of the dislocation density and distribution was observed *in situ* by EBSD after PMT [40]. It has been proven that the kernel average misorientation (KAM) value obtained from EBSD results can be deemed as a semiquantitative description of the local dislocation density [41], as shown in Fig. 4. KAM maps indicated that the in-grain dislocation density became more homogeneous after PMT, and some local high-density areas disappeared. Since there was no magnetostriction effect in the paramagnetic materials, the magnetoplastic effect has been widely accepted to interpret the microstructure modifications induced by PMT.

Interstitial atoms are another kind of point defect besides vacancies, and the dissolution of interstitial atom clusters was also observed in alloys. As a

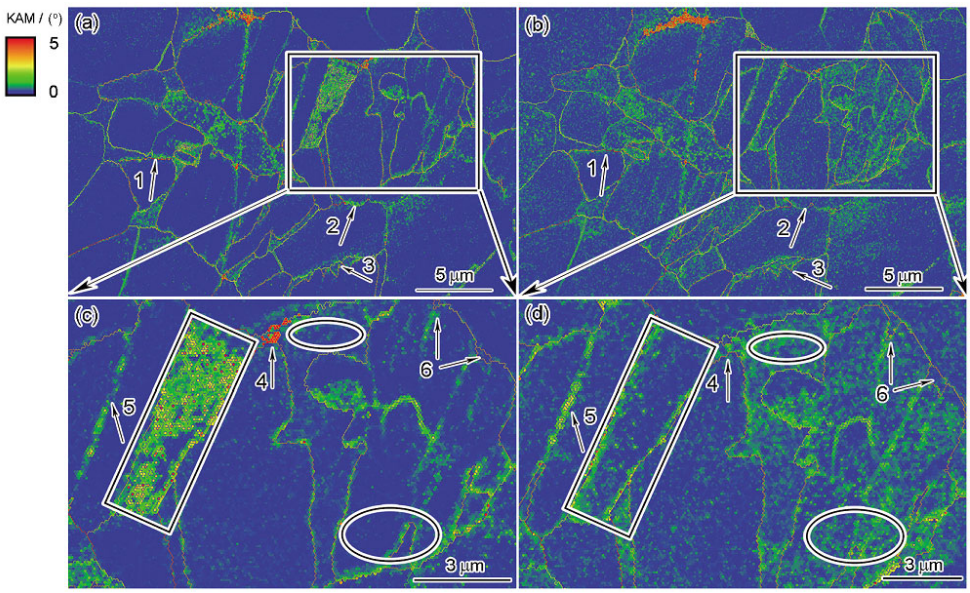

Fig. 4 KAM maps of the Ti-6Al-4V sample before (a, c) and after (b, d) PMT. Obvious variations of the KAM value are marked out. Reproduced with permission from Ref. [40], © Acta Metallurgica Sinica 2019.

common β stable element, Fe is modestly doped into the Ti-6Al-4V alloy. A lot of di-iron cations Fe^{2+} were detected by the secondary ion mass spectrometry (SIMS) tests [42]. Hence, there exist a lot of Fe-rich clusters, bringing about a slight ferromagnetism of the alloy. By excluding the paramagnetic component in the magnetization curves of the Ti-6Al-4V specimens, it can be seen from Fig. 5 that the ferromagnetic saturation magnetizations of the specimens decreased by ~12% after PMT. Therefore, the ferromagnetism of the specimens was significantly weakened, and it suggests that the dissolution of the Fe-rich clusters took place during PMT, which lead to the reduction of the spontaneous magnetic moment of each cluster.

Inspired by the observations in the Ti-6Al-4V alloy, changes in the carbon clusters in the M50 steel were also investigated. Carbon atoms tend to aggregate in the edge dislocation area under the elastic field of the dislocation, which is called the Cottrell atmosphere. Suppose that some of the Cottrell atmospheres dissolve during PMT, these dispersed carbon atoms will diffuse in the martensite and become interstitial atoms. As a result, the lattice distortion rate increases in these areas that the carbon atoms dissolve in, and it was proved by a general decrease in the IQ value after PMT. Besides, the diffraction angle of the $(220)_{Fe}$ face in the X-ray diffraction (XRD) patterns decreased by 0.2° after PMT, corresponding to a larger interplanar distance and a higher lattice distortion rate based on the Bragg Equation [43].

Defects in the metallic glass differ from the crystal due to the irregular atomic arrangement. Atoms are packed less densely than in the corresponding crystal, leaving larger interstitial spaces between atoms, which is called the free volume. The large free volume holes among the atoms are similar to the point defects in crystals as they facilitate atomic diffusion. Few researches were carried out on metallic glasses, but a general conclusion is achieved that PMT promotes the structural relaxation process, making the atomic arrangement more ordered [44, 45]. WC-10Co4Cr coatings are commonly deposited by thermal spraying at a temperature of up to 2,000 °C, and the rapid cooling of the melted Co-binder raises the possibility of metastable amorphous phase. Quantitative characterization of the free volume in the amorphous binders by TEM and positron annihilation lifetime spectra (PALS) indicates that annihilation of the large free volume holes occurred in the binders after PMT owing to structural relaxation (Figs. 6(a)–6(d)). It was also proven by the changes in the XRD patterns [46]. In addition, *in-situ* electron probe microanalysis (EPMA) characterization shows that the distribution of Co became more homogeneous after PMT (Figs. 6(e)–6(h)), which is an analogy to the homogenization effect of PMT on the microstructure of crystal materials.

Surface defects including grain and phase boundaries are another type of defects that widely exist in engineering materials. Due to the discontinuity in composition and structure between two adjacent, much free energy is stored locally. Therefore, in most cases, cracks are prone to initiate at the boundaries, and relaxing the free energy favors the material properties. *In situ* EBSD investigation reveals that the grain boundary characterization distribution (GBCD) of Ti-6Al-4V alloy changed after PMT [40]. Specifically, the fraction of low-angle grain boundaries decreased while the fraction of Σ11 coincidence site lattice (CSL) grain boundaries increased. Dislocation motion near

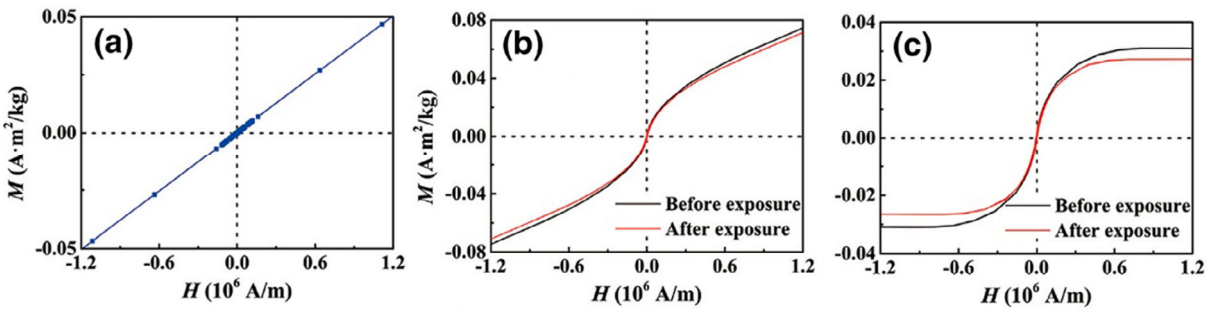

Fig. 5 (a) The magnetization curve of high-purity titanium; (b) the magnetization curves of the Ti-6Al-4V specimen; (c) the ferromagnetic components of the magnetization curve. Reproduced with permission from Ref. [42], © The Authors 2020.

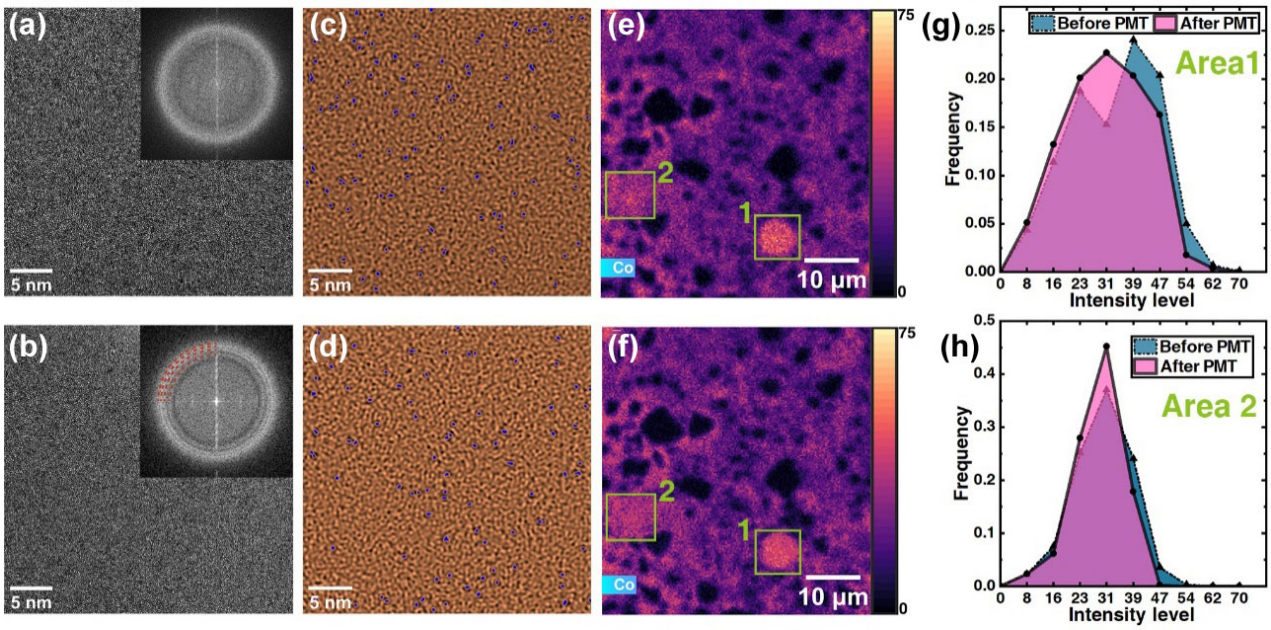

Fig. 6 HRTEM images of the binders in the (a) untreated and (b) PMTed WC-10Co4Cr coating at a magnification of 1.05 Mx; (c, d) distribution of large holes is revealed in the filtered images corresponding to (a) and (b), and the holes are represented by blue; *in situ* Co distribution maps (e) before and (f) after PMT; (g, h) histogram of the intensity level of Co in the area 1 and 2 marked in (e) and (f). Reproduced with permission from Ref. [46], © The Authors 2022.

grain boundaries was deemed to be the cause of GBCD changes in the Ti-6Al-4V alloy. CSL boundaries are more stable than random boundaries as they possess lower interfacial misfits and can offer a more substantial barrier for dislocation transmission under external load. In order to explain the GBCD changes after PMT, further study was carried out on the M50 bearing steel [43]. It was found that the average misorientation angle of low-angle boundaries generally decreased after PMT, while the fraction of CSL boundaries of ferrite, especially the Σ3, Σ9, and Σ11 CSL boundaries, increased (Figs. 7(a) and 7(b)). Most of CSL boundaries are biased from the exact misorientation angle, which results from the linear defects at grain boundaries [47], and the unique property of CSL boundaries will decay with the deviation angle. Changes in the local KAM value are evident in KAM maps before and after PMT, especially at grain boundaries, which indicates that the dislocation motion occurs [43, 48]. In addition, the average deviation angle of different CSL boundaries decreased, as shown in Fig. 7(c). Therefore, it can be inferred that the increased part of CSL boundaries is mainly composed of the grain boundaries identified with a decreased deviation angle rather than the generation of new CSL boundaries, and it is associated with the magnetoplastic effect in essence.

Phase boundaries between WC particles and Co binders are considered the weakest position of the WC-10Co4Cr coating due to the discontinuous atomic arrangement from amorphous to crystalline body, and it can be proved by the frequent observed intergranular fractures in the coating [49]. However, the formation of coherent WC/Co boundaries (Figs. 8(a)–8(c)) was characterized by *in-situ* high-resolution TEM (HRTEM), making the transition of the atomic arrangement smoother. Through molecular dynamic simulations of the different structures, the work of separation of the coherent boundary is found to be much higher than the original disordered one, indicating that the WC/Co boundaries became more stable after PMT (Figs. 8(d)–8(f)). In conclusion, PMT has similar effects on metallic glasses and crystals, that is the microstructure homogenization and interfacial stabilization.

Although the homogenization of defect distribution in both ferromagnetic and non-ferromagnetic materials has been widely reported, the reverse effect of PMT has also been found. For instance, apparent dislocation multiplication, slip and entanglement occurred in the

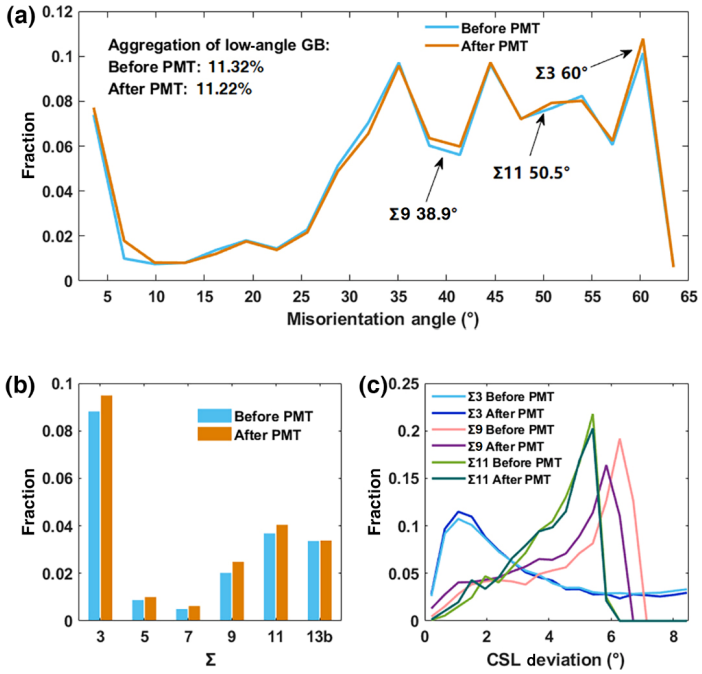

Fig. 7 Grain boundary characterization distribution of ferrite before and after PMT of 0.8 T: (a) misorientation angle distribution, (b) proportion of typical coincidence site lattice (CSL) boundaries and (c) CSL deviations. Reproduced with permission from Ref. [43], © Elsevier Ltd. 2021.

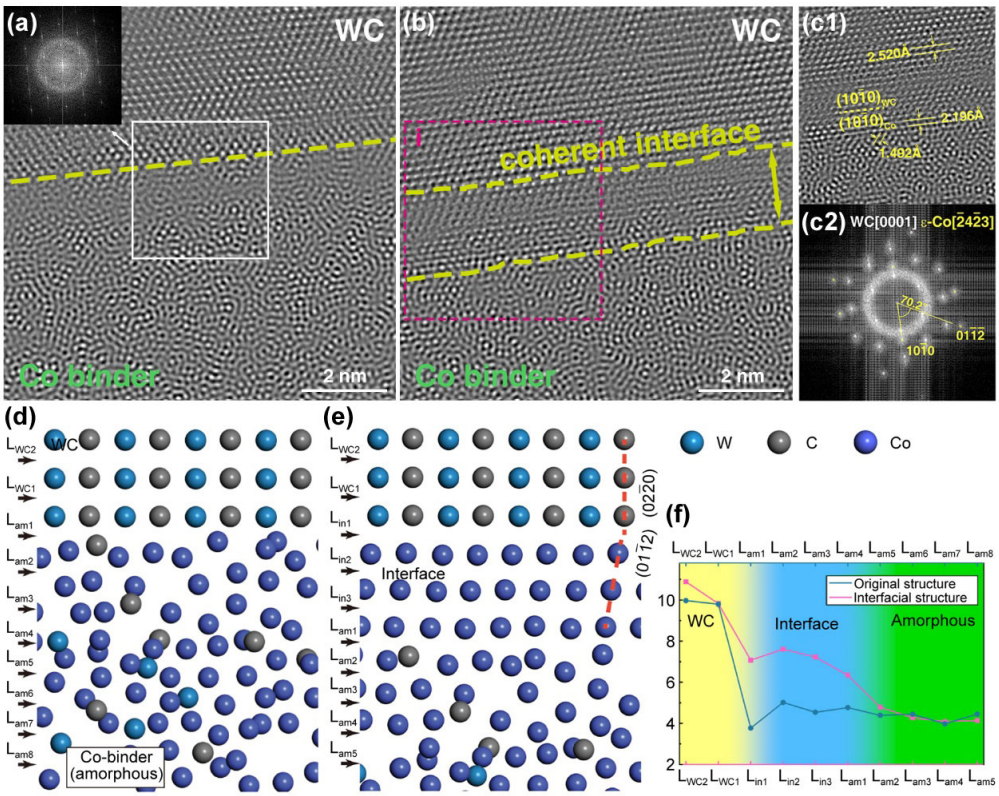

Fig. 8 (a, b) *In situ* HRTEM observation of the WC/Co phase boundary in the WC-10Co4Cr coating; (c1) magnified iFFT image and (c2) FFT pattern of the selected region; molecular dynamics simulation of the boundary: cross-sectional view of atomistic models with (d) disordered and (e) coherent boundaries correspngding to a and b; (f) work of separation at different atomic layers in models. Reproduced with permission from Ref. [112], © Springer Nature 2024.

20Cr2Ni4A steel subjected to the PMT was found by TEM [50, 51]. The increase in the dislocation density of the Ti-6Al-4V alloy treated with 2 T, 3 T, and 4 T magnetic fields was also observed [52]. In addition, the dislocation density in the sample subjected to 3 T PMT was the highest, and the dislocation cell wall structures were observed, as shown in Fig. 9. Similar phenomena have been observed in other materials, including the M50 steel [53], AZ31 magnesium alloy [54], Al matrix composites [55], etc. It is noteworthy that the reverse effect is more commonly reported with a higher magnetic intensity in the research. Hence, there should be an underlying relationship between the extent of the magnetoplastic effect and the magnetic intensity.

2.2 Mechanism for microstructure modifications

Although the observations of microstructure modifications induced by PMT differ in materials, there is a common ground that atomic migration in the defect area is essential. However, the energy brought by the external magnetic field (i.e., Zeeman energy, $\mu_B B=10^3–10^4 kT$, where μ_B is the Bohr magneton, B is the magnetic intensity, k is the Boltzmann constant, and T is the thermodynamic temperature) is almost ignorable compared with the thermal energy at room temperature. From our perspective, atomic migrations induced by PMT are closely related to the break of chemical bonds, and they are by nature kinetic processes similar to the molecular motion during the chemical reaction.

The basic presumption of our viewpoint was derived from the explanation regarding the magnetoplastic effect proposed by Buchachenko [56] and Badylevich et al. [57]. In the NaCl crystals with Ca^{2+} impurity, the pinning is formed due to the Coulomb attractive force between the Cl^- at the dislocation core and the Ca^{2+} at the stopper (pinning point). When the electron transfer from the Cl^- to the Ca^{2+} occurs under the thermal excitation, a short-lived pair of Cl and Ca^+ is formed, along with the disappearance of the Coulomb force, and the pinning effect is "switched off". Governed by the selection rule, the initial and final states have equal spins, that is the singlet state with spin antiparallel. In the absence of the magnetic field, the unpaired electron on Ca^+ will return to Cl in a very short time, "switching on" the pinning effect again. Under the effect of the external magnetic field,

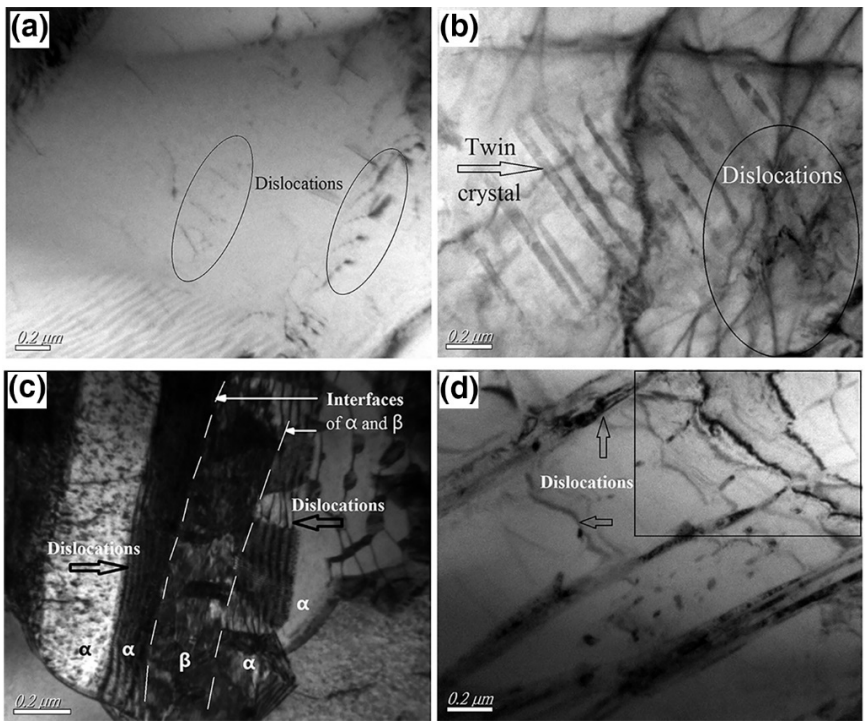

Fig. 9 TEM microstructure of Ti-6Al-4V titanium alloy subjected to magnetic treatment of different intensities: (a) B = 0; (b) B = 2 T; (c) B = 3 T; (d) B = 4 T. Reproduced with permission from Ref. [52], © Elsevier Ltd. 2015.

the two unpaired electrons on Ca^+ and Cl may be transformed to the triplet state, in which case the reverse electron transfer is forbidden according to the Selection rule. Therefore, the switched-off Coulomb force has a longer lifetime, implying a higher efficiency of dislocation depinning. A scheme of such a process is given in Fig. 10(a). Regarding the covalent crystals, Badylevich et al. [57] gave another theoretical interpretation of the phenomenon that the magnetic field has a continuous effect on the plasticity of the monocrystalline Si during the subsequent high-temperature plastic deformation. Some of the point defects in the crystal can be thermally excited. In the meanwhile, the external magnetic field can transform the spin state of the electrons in the point defect from the singlet state to the triplet state, preventing the point defect from deexcitation. With a prolonged lifetime of the excitation state, the point defects tend to relax to some new bonding configuration, hence impacting the plasticity of the crystal in the subsequent deformation.

However, the cause of the spin state transition of the electron pairs in the dislocation pinning center and the point defect was not given in their theories. A commonly accepted theory regarding the electron spin nature might be helpful for interpretation [58–63]. It was originally proposed by the discussion on the influence of the magnetic field on the chemical reaction process. Following is a brief illustration of this theory.

There are two unpaired electrons in an ionized molecule with four possible spin states. Let s represent the total spin quantum number, m_S represent the total magnetic quantum number, and then the four spin states can be described by (s=0, m_S=0), (s=1, m_S=0), (s=1, m_S=1) and (s=1, m_S=–1), respectively. The first state is called the singlet state, while the last three states are called the triplet state. A schematic of the four states is shown in Fig. 10(b) [64, 65]. The spin vector of the electron under the magnetic field will precess in the same direction as the magnetic field, which is called the Larmor precession. The angular

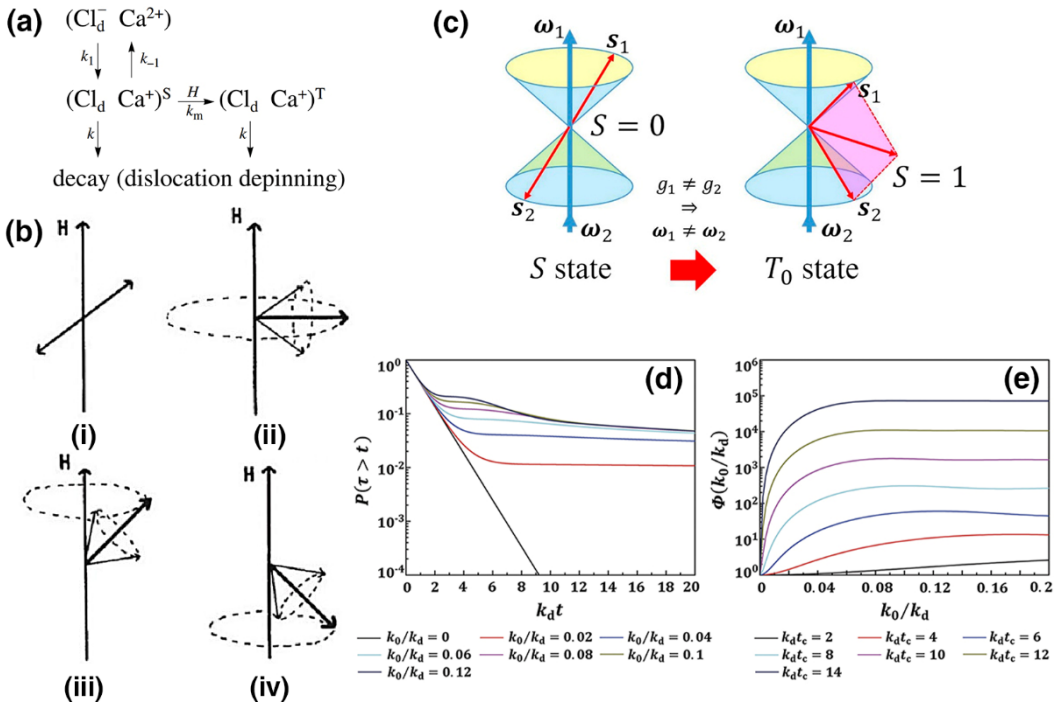

Fig. 10 Mechanism for the magnetoplastic effect. (a) A schematic of the magnetoplastic effect in the NaCl(Ca^{2+}) crystal, where d represents the dislocation, S represents the singlet state and T represents the triplet state; (b) schematic of four spin states of two unpaired electrons: (i) S=0, M_S=0; (ii) S=1, M_S=0; (iii) S=1, M_S=1; (iv) S=1, M_S=-1; (c) a visualized diagram of the Δg mechanism resulting in the spin states transformation; (d) probability distribution of the excited-state lifetime τ; (e) dependence of $\Phi(k_0/k_d)$ on k_0/k_d under different the magnetic flux density B, which reflects the extent to which the atom-migration-related process is promoted. Reproduced with permission from Ref. [8] for (a, b), © Elsevier Ltd. 2008; Ref. [42] for (c), © The Authors 2020; Ref. [69] for (d, e), © IOP Publishing 2021.

velocity of the Larmor precession under the external magnetic field can be written as $\omega = \mu_B g B/\hbar$, where μ_B is the Bohr magneton, g is the Lande factor, B is the magnetic induction intensity, $\hbar$ is the reduced Planck constant, i.e., $\hbar = h/(2\pi)$, and h is the Planck constant. Let S represent the singlet state of the unpaired electron in the reaction system, and T_0, T_+, and T_- represent the triplet states with m_S=0, 1, and –1 respectively, then the S and T_0 states can be visualized as shown in Fig. 10(c). Due to the orbital spin coupling of electrons, the Lande factors of two unpaired electrons may have a slight difference Δg, which results in the difference $\Delta\omega = \Delta g \mu_B B/\hbar$ in the angular velocities of the Larmor precession [66]. Such asynchronous precession of two electrons eventually leads to the intersystem crossing between the S and T_0 states with a frequency of $\Delta g \mu_B B/h$, therefore it is known as the Δg mechanism.

Based on the assumption of the formation of the free radical pair between the dislocation and the adjacent pinning center [59, 67, 68], the Δg mechanism has been widely adopted to explain the causes of magnetoplastic effect [57, 58, 61]. However, it should be noted that, according to the Δg mechanism, transition from the singlet state to the triplet state is also promoted, and it should also be taken into consideration [60]. A more detailed theoretical analysis was employed to obtain the density matrix of four spin stats under the external magnetic field [69]. By calculation, the magnetoplastic effect was no longer attributed to the extended average life of the excited state of the reaction system caused by the external magnetic field, but to the change in the probability distribution of the life of the excited state. Briefly put, the probability that the life of the excited state is longer than the characteristic time of the atom-migration-related process (during dislocation depinning, structure change of point defects, etc.) increases under the magnetic field, as shown in Figs. 10(d) and 10(e).

Here, an explanation for the dissolution of the atomic clusters observed in the M50 steel was given based on Buchachenko's theory. Dislocations are pinned by the Cottrell atmosphere under the elastic, electric and chemical effects. When the electron of the obstacle, e.g., the carbon atoms, is transferred to the dislocation core, bond-breaking occurs between the obstacle and dislocation core. It will in turn change the chemical environment of the obstacle point. Under the magnetic field, the unpaired electrons could be transferred to the triplet state, and it is more likely that some unstable carbon atoms could gradually escape the dislocation area via atomic migration among adjacent sites and diminish the pinning effect of the Cottrell atmosphere. As a result, dislocation motion could take place under the driving force of the residual stress. A schematic illustration of this process is given in Fig. 11(a).

Regarding the covalent crystals, another theory proposed by Badylevich can be further extended to interpret the structural relaxation process in the binder of WC-10Co4Cr coating during PMT [46]. Metallic bonds and covalent metalloid bonds commonly bind atoms in metallic glass. The electrons of the covalent

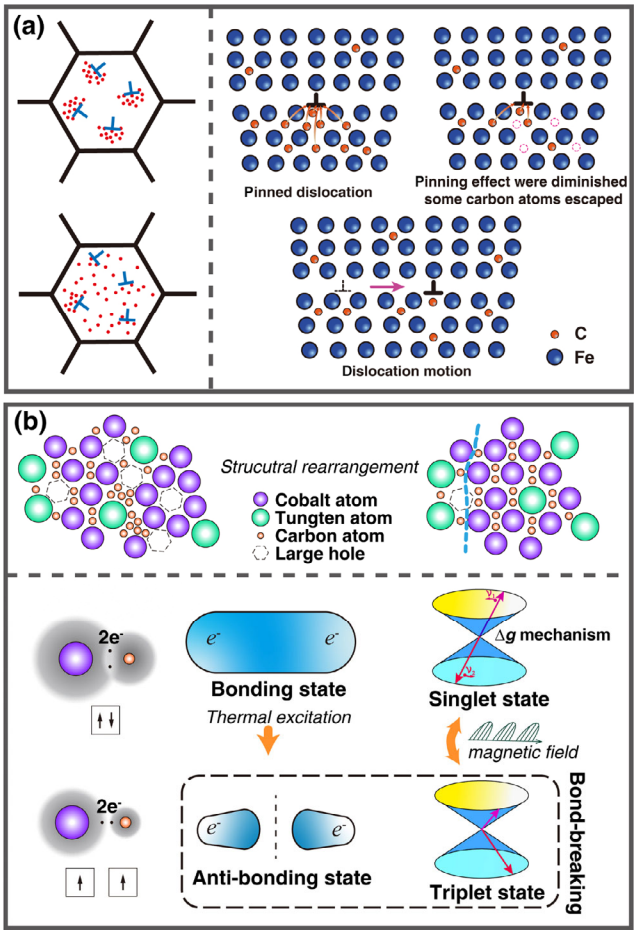

Fig. 11 (a) A schematic illustration of the atomic cluster dissolution and dislocation motion in the M50 steel induced by magnetic field; (b) a schematic illustration of the structural relaxation in the Co-binders of the WC-10Co4Cr coating induced by magnetic field. Reproduced with permission from Ref. [46], © The Authors 2022.

bonds are predominantly in the bonding state, and they may occasionally be excited to the nonbonding or anti-bonding state for a rather short time. During PMT, intersystem crossing between singlet state and triplet state occurs according to the Δg mechanism, and the probability that the excited state lifetime exceeds the critical time needed for the elementary reaction of the bond-breaking process dramatically increases. As a result, atomic migration will take place under the driving force of microcosmic residual stress after bond-breaking. The annihilation of free volume defects was also observed, and it is due to the generation of plenty of unstable dangling bonds captured by the deformation potential around free volume clusters. A schematic illustration is given in Fig. 11(b).

In order to quantify the effect of PMT on defects as far as possible, a first-order equation originally used in chemical reaction kinetics has been introduced to describe the defect density changes during PMT in Eqs. (1) and (2) [46]:

$$\frac{\mathrm{d}c_\mathrm{f}}{\mathrm{d}t} = kc_\mathrm{f}(c_\mathrm{f} - c_\mathrm{eq}) \tag{1}$$

$$k = A\exp\left(\frac{\Delta S}{R}\right)\exp\left(-\frac{\Delta H}{RT}\right) \tag{2}$$

where c_f is the concentration of the defect at time t, c_eq is the concentration of the defect in equilibrium status at room temperature T, k is the reaction rate, A is the natural period of the atom vibration, R is the ideal gas constant, ΔS and ΔH are the entropy and the enthalpy of activation, respectively. Considering that the entropy and enthalpy of activation should not be affected by the pulsed magnetic field since the fundamental process of atomic migration remains unchanged, it can be inferred that the promotion of the atom vibration frequency accelerates the reaction rate during PMT. The atom vibration frequency is further affected by the bonding states within the atom cluster under the fixed temperature. This equation only gives a rough description of the law of defect density changes under the magnetic field, as it only considers the defect annihilation rather than the defect motion. Moreover, the intersystem crossing between the singlet and triplet states needs to be addressed.

A more detailed analysis starts from the spin configuration representation [69]. Omitting the initial derivation, the density matrix $\hat{\boldsymbol{\rho}}(t)$ of the spin states (S, T_0, T_+, T_-) can be written in Eq. (3):

$$\hat{\boldsymbol{\rho}}(t) = \begin{bmatrix} a & -ic & & \\ ic & b & & \\ & & d & \\ & & & e \end{bmatrix} \tag{3}$$

and let $\boldsymbol{u} = [a\ b\ c\ d\ e]^\mathrm{T}$. Then the vector $\boldsymbol{u}$ at any time t meets with Eqs. (4) and (5):

$$\boldsymbol{u}(t) = \mathrm{e}^{\boldsymbol{D}t}\boldsymbol{u}(0) \tag{4}$$

$$\boldsymbol{D} = \begin{bmatrix} -k_d & & \Delta\omega & & \\ & -k_1 & -\Delta\omega & 0.5k_1 & 0.5k_1 \\ -0.5\Delta\omega & 0.5\Delta\omega & -0.5k_\mathrm{d} - 0.5k_1 - k_2 & & \\ & 0.5k_1 & & -k_1 & 0.5k_1 \\ & 0.5k_1 & & 0.5k_1 & -k_1 \end{bmatrix} \tag{5}$$

where k_d is the de-excitation rate of the singlet state, k_1 and k_2 are the frequencies of the longitudinal and transverse relaxation, respectively. Supposing that the excited electron pairs are all in the singlet state at first time, then it is obvious that the initial value $\boldsymbol{u}(0) = [1\ 0\ 0\ 0\ 0]^\mathrm{T}$. Hence, the concentration of different spin states at any time can be obtained, and the defect density can be further calculated by Eq. (6) [70]:

$$\frac{\mathrm{d}c_\mathrm{f}}{\mathrm{d}t} = k(a + b + d + e) \tag{6}$$

It can be found that the defect motion rate is also related to the concentrations of the four spin states, which are magnetic-intensity-dependent variables.

Coupled with microwave, the effect of magnetic field on spin states can be enhanced. Specifically, resonance absorption will occur if the electron spin resonance (ESR) condition is satisfied in Eq. (7):

$$h\nu = \Delta E \tag{7}$$

where h is the Plank constant, ν is the microwave frequency, and ΔE is the energy gap between the electron in different spin states. At this time, the intersystem crossing will be further promoted, and it

can be quantified by introducing a coefficient k_{MV} in Eq. (5), which represents the frequency of spin state transition induced by the microwave. The ESR effect was also verified in monocrystalline silicon samples. Dislocations were introduced on the surface of the monocrystalline silicon through scratching, and then these samples were subjected to PMT and PMT coupled with microwave (MPMT), respectively. The microwave frequencies all met the ESR effect according to different magnetic intensities. Dislocations originally aggregated at the scratch edge were revealed by *in situ* EBSD to move towards the far end by 0.5–0.9 μm from the scratch after PMT. In contrast, the dislocation mobility was higher during MPMT, and the average moving distance is 99% farer than PMT. Supposing that k_{MV} equals 10^{10} s^{-1} and the magnetic intensity is 0.75 T, MPMT substitute for PMT can enhance the dislocation depinning process by 59%, which is at the same order of the experimental result.

3 Effect of PMT on mechanical properties and its applications

3.1 Effect of PMT on mechanical properties

Atomic migration has been observed after PMT, and it is also expected to alter the mechanical properties of materials at room temperature. A series of complex phenomena in mechanical properties changes have been reported, including hardness [53], tensile strength [71, 72], wear resistance [73], fatigue strength [74, 75], etc. In general, these changes can be summarized into three types: improvement in plasticity, reduced notch sensitivity, and defect sensitivity, and they all resulted from more homogenous microstructure and more stable surface defects. As for the components, PMT can further improve their performance by regulating residual stress for better deformation coordination between different parts, especially at the interfaces.

3.1.1 *Plasticity improvement*

Previous studies mainly focused on the plasticity of materials as it is closely related to the dislocation motion [76]. The phenomenon that the magnetic field can improve the macro plasticity of alkali halide crystals was then reported by Alshits et al. [77–79]. They considered such improvement a macro manifestation of dislocation mobility promotion, from which the magnetoplastic effect was named. The researchers further studied the macroscopic plastic deformation of NaCl crystals by applying the magnetic field and mechanical load spontaneously [34]. It was found that the magnetic field resulted in the early yield of the crystals when the elastic strain was about to reach the yield limit ε_y (Fig. 12(a)). Researchers also found that the magnetic field has a continuous effect on plasticity after the magnetic field removal, and it was first observed in NaCl crystals [34, 60]. As is seen in Fig. 12(b), the mean dislocation paths in the NaCl crystals exposed to the magnetic field of B=1 T under

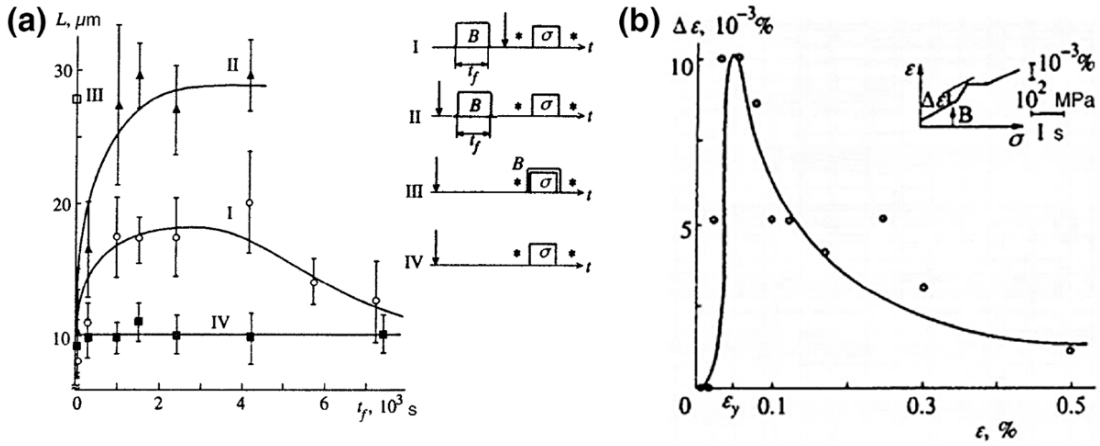

Fig. 12 (a) The deformation jump $\Delta\varepsilon$ caused by a magnetic field pulse of B=7 T in NaCl crystals versus the total deformation of the crystals ε. Inset is a typical deformation diagram at the instant the magnetic field is switched on; (b) dislocation mean free paths of the NaCl crystals under mechanical loading in different situations. The right diagram is the flow chart of the experiment where B represents the magnetic field and σ represents the mechanical load. Reproduced with permission from Ref. [34], © Springer Nature 1999.

mechanical loading are higher than those in untreated ones. In addition, longer exposure times result in larger mean dislocation paths before reaching a constant value. Another group of dislocation-free NaCl crystals was exposed to the magnetic field, and then dislocations were introduced by scratch tests. The mean dislocation paths in such NaCl crystals were also higher than those in the control group under mechanical loading. However, with the increase of exposure time, the mean dislocation paths increased firstly, then decreased. Later, similar magnetic memory effects in monocrystalline Si crystals were reported by Badylevich et al. [57, 80] and Ossipyan et al. [81]. The crystals were exposed to the magnetic field at room temperature and later deformed at over 600 °C. It was found that the starting stress of the dislocation motion decreased [57, 80], and the dislocation mobility was enhanced [80, 81]. The difference in the mean dislocation paths indicated that the magnetic field triggered a series of complex changes in the state of the pinning centers in the crystals.

Plasticity improvement has also been reported in engineering materials, for instance, the Ti-6Al-4V aluminum alloy. The Ti-6Al-4V alloy is widely applied in the aerospace and biomedicine fields, where excellent plasticity and fatigue resistance are required. Therefore, changes in the tensile properties have attracted more attention. Despite slight changes in the elastic modulus, the average yield strength of the solution-treated and aged Ti-6Al-4V alloy [52] decreased from 828.3 to 815.7 MPa, the average tensile strength decreased from 907.7 to 896.3 MPa, and the average elongation after fracture increased from 18.2% to 20.2% after PMT of 2 T. The relationship between the magnetic intensity and the tensile properties was also investigated [52]. It was found that the room-temperature tensile strength was improved after PMT of 2 T and 3 T compared with that of the untreated alloy, while the elongation after fracture was lower. Besides, the variation of tensile strength and elongation after fracture after PMT of 3 T was more evident than that after PMT of 2 T. When the alloy was subjected to PMT of 4 T, both the mechanical properties were improved. Another interesting phenomenon is that the Ti-6Al-4V alloy subjected to PMT of 2 T exhibited different elasticity properties in high-temperature tensile tests. The reduction rate of the elastic modulus increases as the temperature rises, from 9% at 400 °C to 17% at 550 °C. Besides, the plasticity improvement brought by PMT was also more apparent at higher temperatures. The tensile properties of the M50 alloy were also reported to be altered by PMT. According to the analytical results of tensile curves of M50 steel [48], the average tensile strength remained unchanged after PMT. However, the average yield strength decreased from 2,384 to 2,333 MPa, the tensile elastic modulus decreased from 197.4 to 189.6 GPa, and the fracture surface shrinkage rate increased from 2.30% to 3.80%. In addition, the PMTed specimen experienced more plastic deformation before failure, fracturing at a true strain of 6.35%, compared to the untreated specimen that fractured at a true strain of 5.27%. These results all suggest that PMT can improve the plasticity of M50 steel at room temperature.

The plasticity improvement indicates that there is a general increase in dislocation mobility. As mentioned above, the state of the pinning centers is changed after exposure to the magnetic field. Solute atoms aggregating at the dislocation area dissolved through the bond-breaking and atomic migration process. With a large number of dislocations separated from the pinning centers, the pinning effect on the dislocation was also diminished. On the other hand, the dislocations distributed more homogeneously, with some of the dislocation tangles disappearing after PMT. Therefore, the mobile dislocation density under the external load increased, and there was a lower chance for dislocation pile-up, which could avoid blockage during plastic deformation.

The decrease in the elastic modulus of Ti-6Al-4V is also considered to be related to the defect state changes. Under thermal activation, crystal structure defects can cause additional deformation, decreasing the elastic modulus. In metallic materials, the thermal activation behavior of dislocations is the primary cause of additional strain [82, 83]. Specifically, in the Ti-6Al-4V alloy, a dislocation segment between two pinning centers undergoes slip under external force and thermal activation, resulting in dislocation bowing. This process induces a certain amount of additional strain during the elastic stage of high-temperature

tensile tests. Therefore, the additional strain caused by defects is proportional to the dislocation density, as confirmed by both XRD and EBSD results.

3.1.2 *Notch sensitivity elimination*

Notch sensitivity is one of the most significant properties associated with the mechanical behavior of materials [84]. It is used to describe the decreased ductility of the notch tip. A notch concentrates stress and the localized plastic deformation at its tip, where the crack propagates more easily. Therefore, decreasing the notch sensitivity of the materials is beneficial to their service life, and it is also one of the most notable effects of PMT.

Compact tension samples with a prefabricated notch were used to evaluate the fracture toughness K_{IC} and fatigue crack growth rate of materials before and after PMT [48]. It was found that the average fracture toughness of the M50 steel increased by 6.84% from 21.34 MPa·$\sqrt{m}$ of the untreated sample to 22.78 MPa·$\sqrt{m}$ of the treated sample. Meanwhile, by fitting the Paris-Erdogan law, the fatigue crack growth rate of the sample was found to decreased by 33.6% (Fig. 13). SEM observations show that the width of the stretch zone at the crack tip increased after PMT, indicating that the toughness was improved. Overall, PMT can alleviate the notch sensitivity of the M50 steel.

The deformation behavior of polycrystals was determined by the generation of dislocations and the interaction between dislocations and grain boundaries. Grain boundaries can act as a barrier to dislocation transmission while they are also sources of dislocations during plastic deformation. Researches have shown that grain boundaries with lower free energy can provide a stronger barrier against dislocation transmission and elevate the critical stress needed for dislocation generation [85]. Microstructure characterization indicates that the concentration of CSL boundaries significantly increased after PMT, corresponding to a lower interfacial free energy and a more stable support against crack propagation.

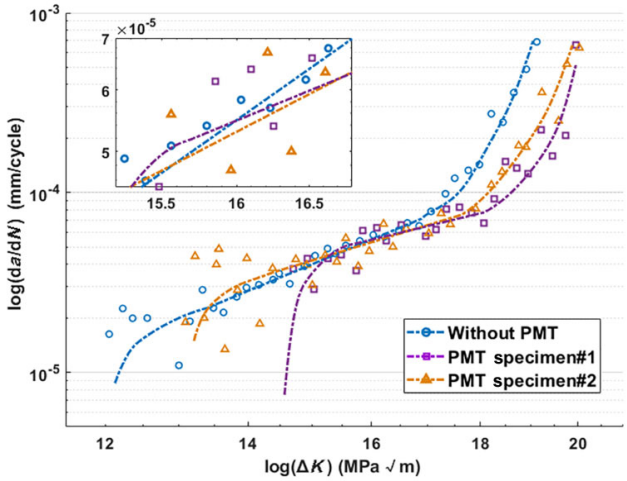

Fig. 13 Fatigue crack growth rate with respect to stress intensity factor of the specimens with and without PMT. Reproduced with permission from Ref. [43], © Elsevier Ltd. 2021.

Fracture toughness is critical for the fatigue life of the WC-10Co4Cr coating, and it was measured through indentation tests. Vickers indentation was used to generate cracks at the four corners of the indentation, and the fracture toughness can be obtained by measuring the crack length. It also represents the notch sensitivity of the coating. As shown in Figs. 14(a) and 14(b), the fracture toughness of the coating increased by 17.7% after PMT [46]. The hardness H and elastic modulus E of the Co-binder in the coating were further tested solely by nano-indentation, and both of them were found to be significantly improved (Figs. 14(c) and 14(d)). The parameter H^3/E^2 representing the fracture toughness of the Co-binder increased by 26.1%, indicating that the main reason for the fracture toughness improvement of the coating lies in the better performance of the Co-binders.

Structural relaxation of the Co-binders after PMT was observed, and it is deemed critical in improving the fracture toughness of the coating. The presence of a high concentration of excess free volume during the initial stages of deformation can significantly reduce the viscosity within the shear bands [86]. Additionally, tensile residual stress, which is widely distributed throughout the binder, can increase local free volume during deformation, resulting in a higher likelihood of microcrack formation with highly localized plastic strain. PMT-induced structural relaxation promotes the annihilation of a certain concentration of large voids, leading to a more dispersed distribution of these voids. Meanwhile, most of these voids remain, allowing for unrestricted nucleation of shear bands.

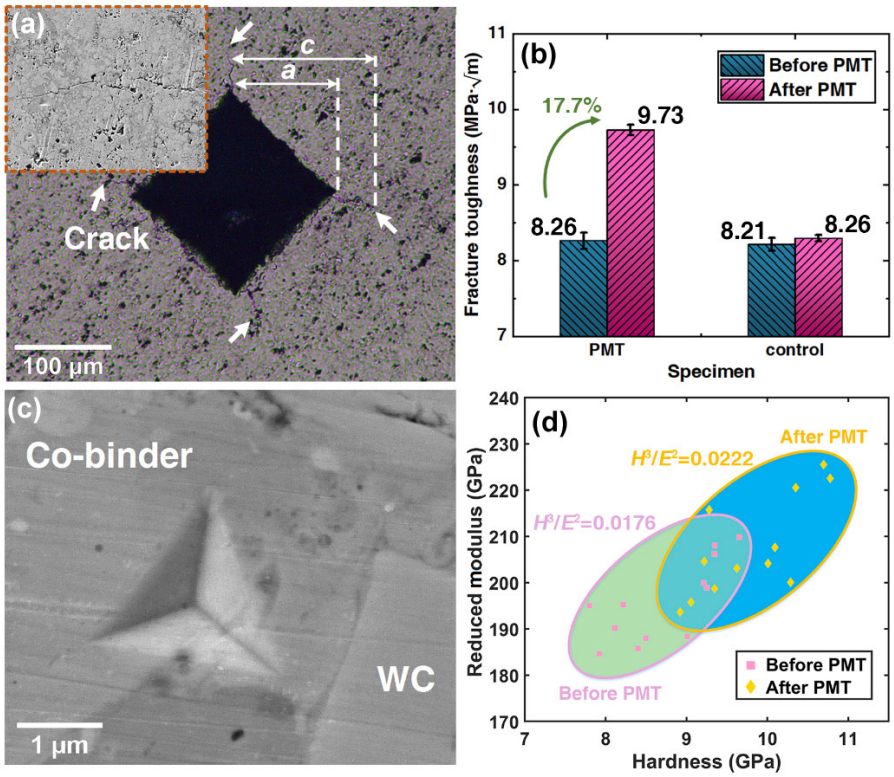

Fig. 14 (a) A typical optical microscopy image of the indentation with cracks at the four corners; (b) fracture toughness with standard error of the specimen before and after PMT. Another specimen was measured two times without PMT under the same condition as control; (c) a typical SEM image of the Berkovich nano-indentation in the binder; (d) hardness and elastic modulus of the binder before and after PMT. Reproduced with permission from Ref. [46], © The Authors 2022.

As a result, the fracture toughness of the coating is improved due to the microstructure modifications of the binder.

3.1.3 *Defect sensitivity elimination*

Defects such as pores and inclusions widely exist in materials. Due to the discontinuity between defects and the matrix, stress concentration tends to occur at their interfaces. Typically, brittle materials fail at stress concentrations due to their high defect sensitivity, especially under the cyclic load [87]. Researchers have shown that PMT can also effectively extend the fatigue life of materials by decreasing their defect sensitivity.

For instance, mechanical properties of bearing steels depend strongly on the type, size, and density of carbides in the matrix. Primary carbides are undesirable in bearing steels due to their large size and high hardness. These carbides are usually difficult to dissolve through heat treatment and often cause fatigue failures [88, 89]. Based on the contact fatigue tests, the service life of the GCr15 sample after PMT was up to 168,969 cycles with the failure probability $P(N)$=10%, and that of the untreated sample was 80,447 cycles [90]. Hence, the rated life of GCr15 bearing steel is increased by 1.1 times after magnetic treatment. The low cycle three-point bending fatigue performance of GCr15 steel was also improved by PMT [36]. The fatigue tests ended at 150,000 cycles, and the number of cycles when cracks initiated was taken as the life index. The results showed that when the load amplitude was 30 kN, the fatigue life of both two groups reached 150,000 cycles. When the load amplitude was increased to 40 kN, the untreated group cracked before 20,000 cycles, while the fatigue life of the treated group still reached 150,000 cycles. When the load amplitude was increased to 45 kN, the fatigue life of the treated group was still significantly higher than the untreated one, though they were both lower than 150,000 cycles. Since the fracture behavior of the PMTed and untreated samples exhibits no difference, it can be inferred that the fatigue and

creep life improvement resulted from the decrease in their defect sensitivity.

The homogenization of the microstructure accounted for the decrease in defect sensitivity induced by the pulsed magnetic field. For one thing, dislocation distributes more evenly after PMT, and the dislocation pile-up is relieved. It is achieved by the dislocation motion from the high-intensity region to the low-intensity region, accompanied by the dislocation annihilation. As a result, the stress concentration induced by the pile-up dislocations will become less prone to formation, improving the defect sensitivity of the material. In addition, the segregation of elements can be relieved through the dissolution of atomic clusters. These atoms will end up as solute atoms in the matrix, and the solid solubility of the solute atoms is thus improved. Such progress will also lead to a more homogeneous concentration of solute atoms in the matrix, and thus, mechanical properties were improved from solid solution strengthening.

PMT has a more pronounced effect on the fatigue and creep performance of the Ti-6Al-4V alloy [72, 75]. The low-cycle fatigue life of the Ti-6Al-4V alloy has been enhanced by about 30% [75], as shown in Fig. 15(a). Further fatigue crack growth tests showed that the fatigue threshold value increased by 7.8% under low stress intensity factor (Figs. 15(b) and 15(c)), while the crack propagation rate remained almost unchanged. Creep tests on PMTed specimens took significantly longer to reach the specified creep strain than untreated specimens under the same conditions, with a maximum relative increase in the creep life of over 200% [72].

Under cyclic loading, the accumulation of dislocations causes hardening at the crack tip and accelerates crack propagation by forming the cell structure. Unlike the as-received sample, fewer dislocation walls were found in the PMTed sample. It can be inferred that dislocations were harder to pile up and form the cell structure after PMT. It is in accordance with the conclusion that the dislocation mobility was enhanced with fewer pinning centers. Besides, the creep property improvement is also believed to benefit from the magnetic-induced dissolution. Fe atoms gathered around dislocations in the β-phase of Ti-6Al-4V titanium alloy facilitate dislocation climb, accelerating the creep damage. During PMT, some of these atomic clusters will dissolve into the matrix, and there is a decreased percentage of dislocations that can climb and escape new obstacles by the fast diffusion of Fe atoms.

3.1.4 *Interface strengthening*

Interfaces widely exist in components made by two or more kinds of materials. Intense thermal and mechanical effects during manufacturing often generate significant residual stresses and uneven residual stress distribution. Excessive residual stress is generally undesirable as it can trigger the crack initiation, especially at interfaces. PMT can be utilized to regulate the residual stress in components at room temperature through microstructure modifications. An outstanding advantage of PMT is its targeting effect, which can relieve the local stress concentration to avoid uneven stress distribution. Therefore, the residual stress relaxation effect on different components with high

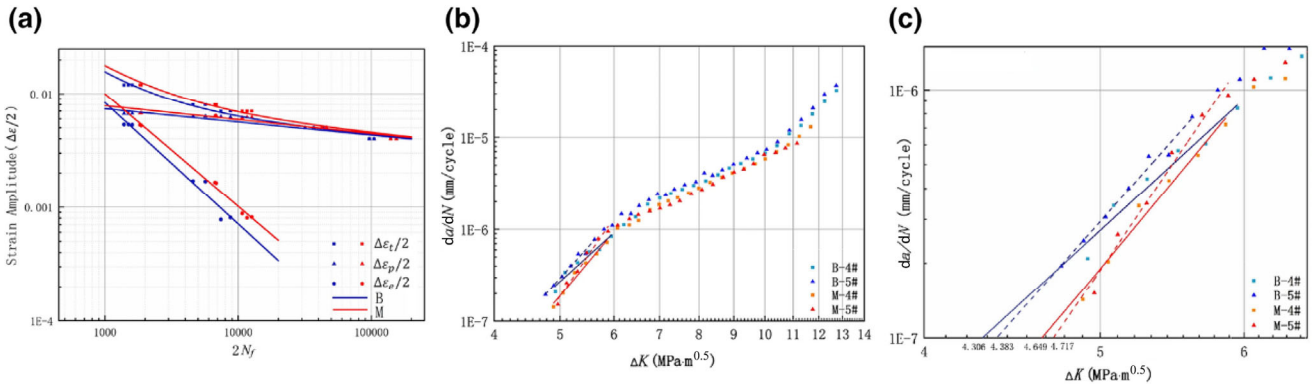

Fig. 15 (a) S-N curves of the untreated (B) and PMTed (M) specimens in low-cycle fatigue tests; (b) fatigue crack growth rate of the untreated and PMTed specimens in the fatigue crack initiation period and (c) a magnified image used to fit the fatigue threshold. Reproduced with permission from Ref. [75], © Springer Nature 2023.

residual stress levels has been investigated [91, 92], for instance, the welding joints and coatings.

The law of the residual stress relaxation on welding residual stress was studied in detail. Lu et al. [93] investigated the effect of the single and multiple magnetic field pulses on the residual stress in restraint low-carbon steel and welded HT50 high-intensity steel. Residual stress in both specimens decreased after treatment, and the multiple pulses had a more remarkable effect on residual stress relaxation than the single pulse. In the same year, they also found that the low-frequency alternating magnetic field treatment can release the residual stress in welded HT50 and HT70 steel [94]. Similar results were also reported in the 30CrMnSiA steel [35]. Further, the extent of the relaxation effect also correlates to the direction of the magnetic field [95–97]. Specifically, the effect was most efficient when the magnetic field was perpendicular to the direction of the principle stress, while it was relatively small when they were parallel [95]. Regarding the welding joints made of QStE420 steel, it was also found that the magnetic field applied perpendicular to the weld bead could release the longitudinal stress significantly. In contrast, the effect is relatively small when the magnetic field is applied parallel to the weld bead [98].

The release of the residual stresses was also found to correlate with the initial stress level of the specimens. The amplitude of the residual stress relaxation in the specimen with higher initial stress was greater than that in the specimen with a low initial stress level (Fig. 16(a)). In particular, the residual stress almost remained unchanged after PMT in the annealed specimen [96]. For the uneven residual stress distribution in the welding joints, similar results were drawn that the residual stress in the region with low initial stress decreased slightly after PMT, while that decreased significantly in the region with initial stress concentration [99], as shown in Figs. 16(b) and 16(c). Despite the previous research which revealed that the magnetostriction effect was not the sole factor [37], the directionality of the effect of the PMT indicates that the magnetostriction effect does play a role in the process of residual stress relaxation. In addition, a new method has been proposed to predict the degree of residual stress relaxation according to the magnitude of the magnetostriction coefficient [97].

Coatings are widely used in machining tools, which involve depositing a layer of coating in several microns on the tool surface, and they play a critical role during friction [100]. Different from the atomic connection in welding joints, mechanical bonds commonly form between the coating and substrate. Therefore, residual stress plays a critical role in the adhesion strength. Scratch tests were applied to study the effect of PMT on the adhesion strength between the cemented carbide and AlCrN coating on the coated cemented carbide tools [101, 102]. After PMT, the adhesion strength between the coating and substrate was significantly increased by about 35%, and the friction coefficient of the indenter was significantly reduced. The milling experiments indicate that tools with PMT possess better wear capacity and lower cutting forces due to the higher cohesion strength [103]. From the alterations in debris shape and size during the scratch test, it can be concluded that

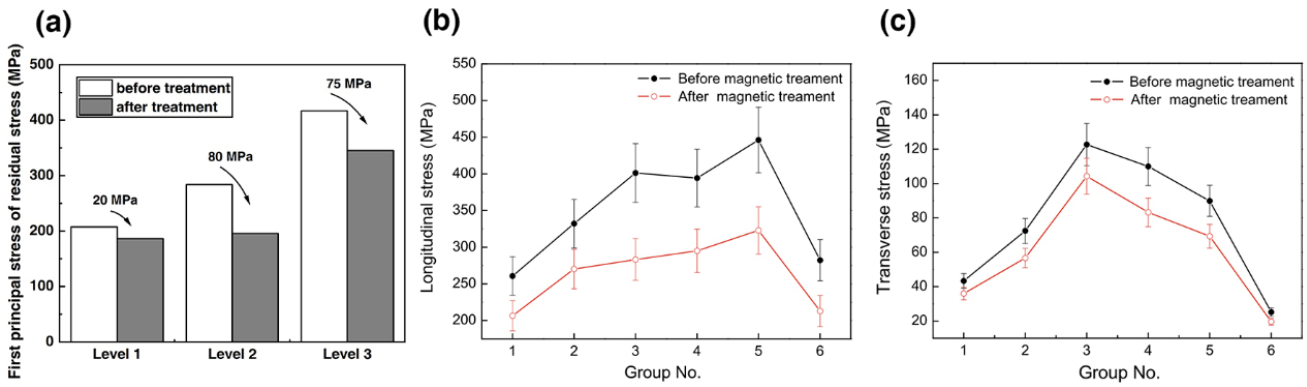

Fig. 16 (a) Residual stress relaxation in specimens with different initial stress levels [96]; (b) comparison of longitudinal stress σx and (c) transverse stress σy in the welding bead before and after magnetic treatment. Reproduced with permission from Ref. [99] for (b, c), © Elsevier Ltd. 2012.

PMT modifies the residual stress distribution at the interface. Elastic energy is prone to accumulation in the front section of the indenter.

Coatings on machining tools are commonly too thin to conduct residual stress measurements. Hence, the thermal sprayed WC-10Co4Cr coating with a 150 μm thickness is adopted for further investigations. The residual stress distributes unevenly in the thermal sprayed coating due to the combination of the thermal mismatch, peening, and quenching effect [104]. *In-situ* residual stress measurements were carried out by XRD with a microfocus X-ray (IμS) source [105]. As shown in Fig 17(a), ablation craters made by the femtosecond laser were employed for repeated positioning before and after PMT. Both tensile stress on the surface and compressive stress in the interior and interface regions decreased dramatically after PMT (Fig. 17(b)), which cut the huge residual stress gap along the depth direction by 1 GPa. Meanwhile, the residual stress gradient along the transverse direction was also effectively relieved.

Scratch tests were applied to evaluate the residual stress relaxation effect on mechanical properties of the coating. Owing to the high thickness of the coating, cross-section scratch tests were conducted on the cross-section of the coating and substrate before and after PMT. The geometric characteristics of the scratches were measured after scratch tests (Fig. 17(c)). Adhesion strength of the coating is inversely correlated to the crack length at the interface, whereas the cohesion strength is inversely correlated to the projected cone area [106]. The average crack length decreased by 20.46%, and the projected cone area also decreased by 16.64% after PMT (Fig. 17(d)). Therefore, the adhesion and cohesion strength of the coating were improved after PMT.

In contrast to the common opinion that higher compressive stress in materials favors fatigue performance, researches have shown that tensile stress in the coating causes through-thickness microcracking, while compressive stress tends to promote microcrack propagation along the interface [107, 108]. Excessive stress gradient also leads to failures, including the buckling, delamination, and warping of the coating. Plastic deformation coordinates better among the interface as the residual stress distributed more evenly after PMT, and the superimposition of the residual stress and external load is less prone to excessive

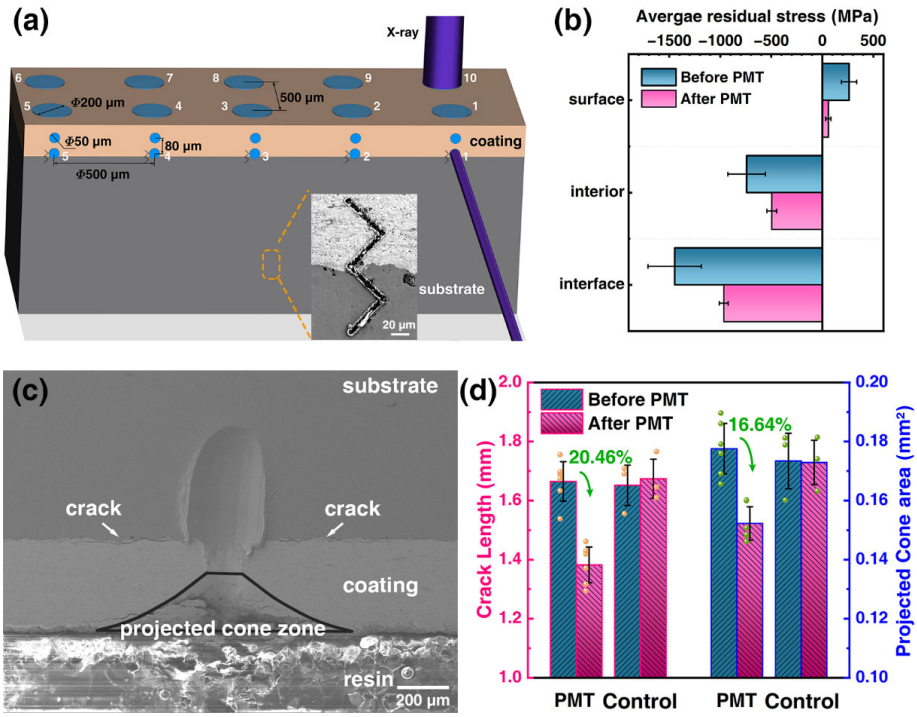

Fig. 17 (a) A typical SEM image of the cross-section scratch; (b) geometric characteristics of the scratches before and after PMT; (c) a schematic illustration of the *in situ* residual stress measurement; (d) average residual stress in different regions of the coating. Reproduced with permission from Ref. [105], © Springer Nature 2024.

stress concentration. Therefore, the adhesion strength between the coating and substrate was enhanced.

3.2 Applications of PMT

PMT exerts a comprehensive strengthening effect on the mechanical properties of materials at room temperature. Hence, it can be treated as an enticing post-treatment method for engineering parts to improve their service performance and life at room temperature, especially for precision parts. Some typical and successful applications are to improve the tribological performance of bearings and machining tools.

3.2.1 Applied research on service reliability improvement of bearings

Bearings are one of the most important components in tribomachinery and are widely used in automobile, railway transportation, aerospace, military and other industries. As a fundamental part, its manufacturing quality is of great significance to the equipment's accuracy, performance, life, and reliability [109, 110]. Due to the constant friction between the rollers and raceways during service, rolling contact fatigue is the primary mode of bearing damage, especially on the inner ring [111]. Researches on the effect of PMT on aeroengine bearings have been conducted based on the rolling contact fatigue tests. The dispersion of the fatigue life decreased significantly, representing a higher reliability of the bearing. As shown in Fig. 18(a), the L_5 life (with a failure probability of 5%) of the untreated bearing was approximately 2.5×10^6 cycles, while that of the treated bearing was up to 1.2×10^7 cycles, which corresponds to a 5 folds increase in the fatigue life, taken the shape parameter β of the Weibull distribution as an index of the dispersion of fatigue life, β_0=1.01 for the untreated bearing, while β_m=3.20 for the treated bearing. Therefore, PMT can effectively decrease the dispersion of fatigue life, and it is especially significant for applications requiring high reliability. In addition, the effect of PMT on different types of GCr15 thrust needle roller bearings (including NRB-931, NRB-932, NRB-936, NJ306X3WB/C9, etc.) has also been investigated based on the single durability bench tests. The service life of bearings subjected to PMT has increased by more than 300%, and the strengthening effect is stable for various kinds of bearings (Fig. 18(b)). By now, PMT has been batched into engineering application to improve the life and reliability of bearings.

3.2.2 Applied research on cutting performance improvements of machining tools

Tool wear is a primary concern in machining, which affects not only the machining efficiency and cost but also the quality of the machined components [112], and the application of PMT has been proven effective to improve the wear resistance and cutting performance of various types of machining tools [112]. Under the same cutting conditions, the tool life of the untreated tool was 86 steel parts at most, while it was up to 127 parts for the tool subjected to PMT. Besides, as shown in Figs. 19(a)–19(e), the treated tool had a lower wear content than the untreated one. The wear morphology and element content at the untreated and treated tool tips were analyzed by SEM. It was found that the

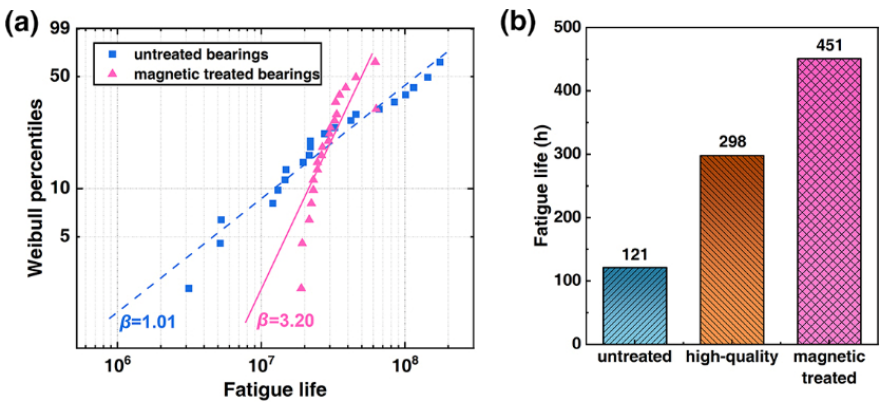

Fig. 18 (a) Rolling contact fatigue life of magnetic treated and untreated M50 steel bearings; (b) single durability bench test results for untreated, high-quality, and magnetic treated bearings.

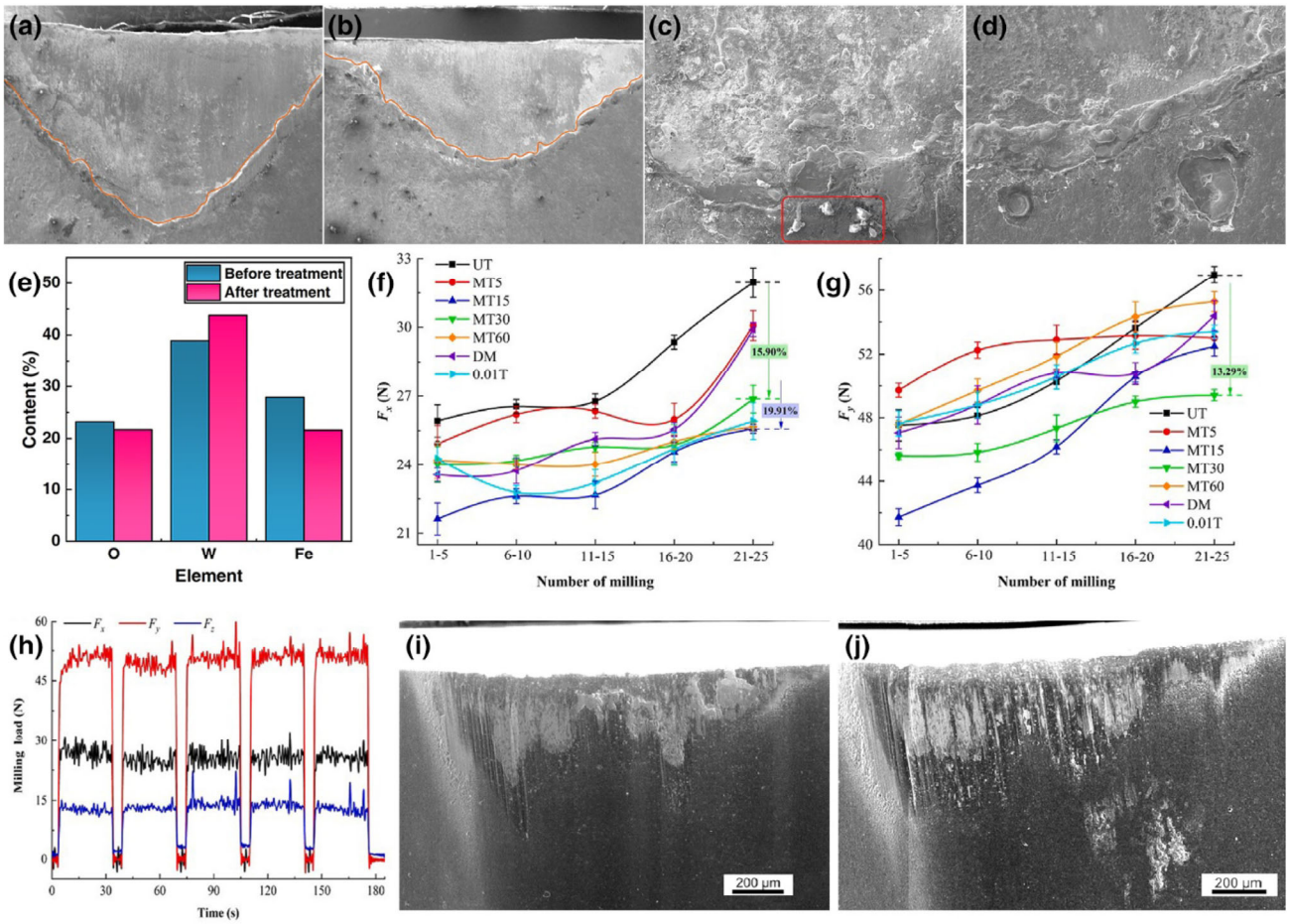

Fig. 19 Friction comparison of tools subjected to magnetic treatment. Wear morphology on the flank face of the cemented carbide tools: (a, c) before magnetic treatment; (b, d) after magnetic treatment. (e) Element content of the wear region. Curves of resultant forces in the *x*, *y* directions, (f) F_x, (g) F_y and (h) join milling forces of five times milling. Eight types including untreated (UT), magnetic treated of B=1.5 T for 5, 15, 30, 60 seconds (MT5, MT15, MT30, and MT60), magnetic treated of B=0.01 T and demagnetized (DM) tools were used. Wear morphology on the flank face of the CBN tools before (i) and after (j) pulsed magnetic treatment [70]. Reproduced with permission from Ref. [115] for (f–h), © Elsevier Ltd. 2022.

edge of the wear scar on the untreated tool tip was blurry with many bonded iron oxides. In addition, there were many built-up edges in the wear scar. In contrast, the wear morphology of the treated tool was sharp with fewer built-up edges in the wear scar. There was less steel adhered to the wear scar, and the content of Fe in the wear region on the rear tool face was reduced by 28%. It can be inferred that PMT reduces adhesive wear during cutting and improves the wear resistance of the coating on the machining tool. In 2019, Xu [101] researched the influence of PMT on the cutting performance of various coated carbide tools. Cutting experiments were performed on different materials, including 45# steel, Ti-6Al-4V titanium alloy, 65Mn steel, etc. The results showed that the wear of tools was alleviated after PMT with specific parameters, and the service life was extended. It was also found that the milling force, including F_x, F_y, and the join forces (Figs. 19(f)–19(h)) were decreased using the PMTed tools, and the surface roughness of the workpiece also decreased in contrast to the control group [114–118]. The reduction of adhesive wear and the attraction of acceptable wear debris by the remanence contributed to the transition from two-body to three-body friction [115]. Therefore, the cutting performance of the coated cemented carbide tools was improved.

PMT has also been proved effective in reducing the adhesion wear of the cubic boron nitride (CBN) tools during machining [70, 102]. As shown in Figs. 19(i)

and 19(j) [70], the adhesive layer occurred with protruding adhesives on the flank face of the CBN tool when cutting cast iron. The element analysis showed that the main elements of these adhesives were Fe and C, indicating that they were derived from the material peeled off from the workpiece. After PMT, the overall degree of adhesive wear on the flank face was reduced. The morphology of the adhesive manifests itself as a flat layer with only a protruding adhesive observed far from the edge. The smooth and flat adhesive layer corresponds to a slighter adhesive wear, which has slight damage to the surface integrity of the workpiece and tool, and it can even act as a lubricant to protect them from wear [119, 120]. In contrast, the adhesive with irregular and the protruding surface indicates that the firm bonds were formed at the stick points. It will not only lead to the peeling of large pieces from the workpiece but also cause wear and scratches on the surface of the workpiece in the subsequent machining. In conclusion, the blocky adhesives on the flank face of the CBN tool were reduced, and the adhesive wear was relieved after PMT.

3.2.3 *Combined applications of PMT*

By regulating defect states in the material, PMT can be coupled with other methods to improve their treatment effects to a greater level. Deep cryogenic treatment (DCT) is a special kind of heat treatment, and the pulsed magnetic field coupled with DCT (MDCT) was studied [121, 122]. It is known that deep cryogenic can promote the martensitic transformation from the retained austenite. However, the phase transformation was found to be inhibited by MDCT. In the experiment, the retained austenite in the quenched M50 steel decreased by 10% after DCT, while it only decreased by 3% after MDCT [122]. The dissolution of carbon clusters was introduced for explanation. The carbon atoms in the martensite dissolved near the phase boundaries can easily migrate to nearby austenites by following the moving dislocations. It will improve the carbon content and stability of retained austenite, retarding the martensite transformation.

Laser shock peening is widely used in mechanical property improvements of metallic materials, and the nonuniformity of the treatment effect is one of the major concerns. Through the novel method of magnetic-field-assisted femtosecond laser shock peening (MFLSP), a more uniform grain refinement effect with a higher area fraction of small grains was achieved in the Ti-6Al-4V alloy [123], as shown in Figs. 20(a)–20(d). Surface hardness also distributed more uniform in spite of a slight decrease compared to the normal laser shock penning, as shown in Fig. 20(e). *In situ* EBSD tests have shown that dislocation lines dispersed from low-angle grain boundary to the intragranular area, and they could serve as potential dislocation sources for the grain refinement during laser shocking. This attempt paved way for new possibilities of homogenous mechanical property improvements.

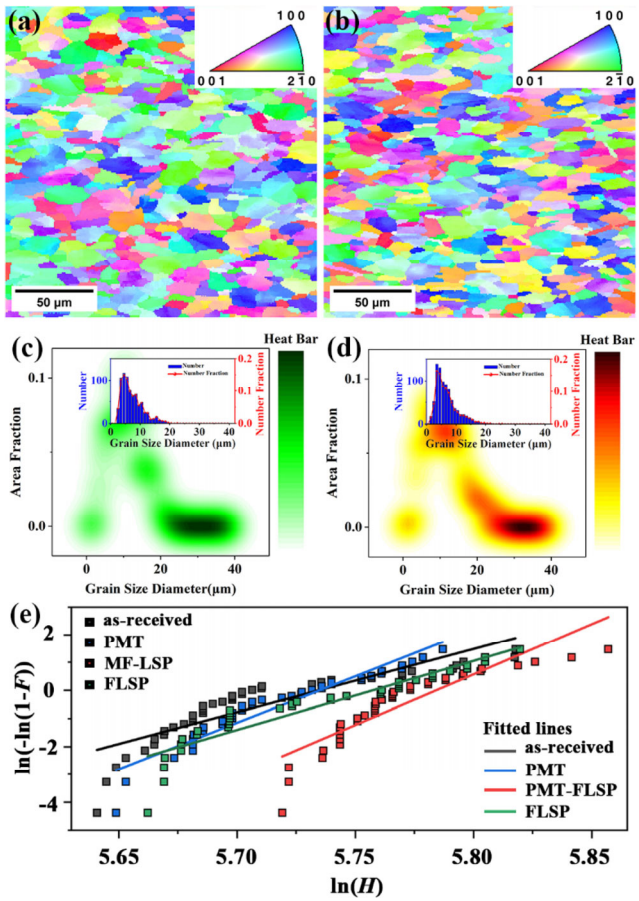

Fig. 20 Inverse pole figures of (a) femtosecond laser shock peenning (FLSP) and (b) MFLSP samples; heat maps of the grain size distribution for the (c) FLSP and (d) MFLSP samples; the inset histograms representing the changes in grain numbers and fractions with respect to grain size diameters; (e) weibull distribution analyses of the surface hardness of different samples. Reproduced with permission from Ref. [123], © Wiley 2023.

4 Conclusions

The appeal of PMT lies in its simplicity and ability to regulate the microstructure and mechanical behavior of materials at room temperature without affecting the size accuracy and surface quality. The current industrial application of PMT is mainly focused on machining tools and bearings and has achieved satisfactory results in improving of service reliability in various products. It is inseparable from a thorough understanding of the fundamentals of PMT.

Among the proposed theories, the magnetoplastic effect is the most widely accepted by the researchers. It is closely related to the behavior of point, line and face defects under the external magnetic field, and has been verified in all kinds of material systems. However, it has been long-term debated on the mechanism of the magnetoplastic effect, i.e. the reason for the defect state change when exposed to the magnetic field. It is mainly due to the great difficulty in directly observing the changes of valence electrons under the action of the external magnetic field.

There have been frequent reports on the effect of the pulsed magnetic field on the microstructure of structural materials. The dislocation-related phenomenon, including dislocation motion, multiplication and annihilation, is commonly reported in particular, which is the intuitive reflection of the magnetoplastic effect. Most of the researchers gave an interpretation of the residual stress changes and mechanical property improvement based on the microstructure modifications. However, since tribological behavior is a comprehensive action of multiple factors, an explicit theoretical explanation that chains the microstructure modifications, residual stress, mechanical properties in series is still sparse.

On the other hand, with a better understanding on the regularity of the effect of PMT on wear resistance and its mechanism, PMT has been industrialized and rolled out more widely in the manufacturing process of many precision parts and components. The further promotion of PMT relies on the forward design for ideal tribological performance by regulating the microstructure, residual stress, and mechanical properties through the specific pulsed magnetic field. However, uncertainties in the essence of the magnetoplastic effect pose a severe barrier to the quantitative characterization of defect changes under the magnetic field with specific parameters, and it is hard to predict the corresponding strengthening effect. Fortunately, the rapid development of density functional theory (DFT) makes it possible to understand the relationship between the changes in electron spin configuration and the state of defects under the magnetic field. Once the general laws for the magnetoplastic effect in different kinds of materials are achieved by the DFT simulation, not only the theoretical system but also the industrialization of PMT is expected to be vigorously promoted.

In conclusion, PMT has achieved periodic success from the perspective of applications, while more challenges are still ahead. One is that the mechanism for the strengthening effect of PMT is still in the exploring, and the other is it still desires the significant breakthrough in the detection methods. Promoting the PMT to the precision parts with complex and extreme service conditions has become the bottleneck of the PMT application that has to be broken through, and it depends on the close combination of practice and in-depth research.

Acknowledgements

The authors gratefully acknowledge the financial supports from National Key R&D Program of China (No. 2020YFA0714900), Joint Fund of the Ministry of Education (No. 8091B012201), and National Natural Science Foundation of China (No. 52031003).

Declaration of competing interest

The authors have no competing interests to declare that are relevant to the content of this article.

References

[1] Davidson P A. Magnetohydrodynamics in materials processing. *Annu Rev Fluid Mech* **31**: 273–300 (1999)

[2] Eckert S, Nikrityuk P A, Räbiger D, Eckert K, Gerbeth G. Efficient melt stirring using pulse sequences of a rotating magnetic field: Part I. Flow field in a liquid metal column. *Metall Mater Trans B* **38**(6): 977–988 (2007)

[3] Gheorghies C, Stefanescu I I. Effects of thermomagnetic treatment on microstructure and mechanical properties of rolling bearing steel. *J Iron Steel Res Int* **17**(9): 46–52 (2010)

[4] Wang F, Qian D S, Hua L, Mao H J, Xie L C, Song X D, Dong Z H. Effect of high magnetic field on the microstructure evolution and mechanical properties of M50 bearing steel during tempering. *Mater Sci Eng A* **771**: 138623 (2020)

[5] San Martin D, van Dijk N H, Jiménez-Melero E, Kampert E, Zeitler U, van der Zwaag S. Real-time martensitic transformation kinetics in maraging steel under high magnetic fields. *Mater Sci Eng A* **527**(20): 5241–5245 (2010)

[6] Dong B Q, Hou T P, Wu K M, You Z Q, Li Z H, Zhang G H, Lin H F. Low-temperature nanostructured bainite transformation: The effect of magnetic field. *Mater Lett* **240**: 66–68 (2019)

[7] Vorob'ev R A, Dubinskii V N. Effect of treatment by a pulsed magnetic field on the hardness and fracture strength of a hypereutectoid tool steel. *Phys Metals Metallogr* **115**(8): 805–808 (2014)

[8] Miller P C. A look at magnetic treatment of tools and wear surfaces. *Tool Prod* **55**(12): 100–103 (1990)

[9] Peter K. Tool life grows in mangetic fields. *Mach Prod Eng* **147**(3762): 78–79 (1989)

[10] Tang, X R, Wei, Z C, Jing, X W, Xu, S F, Chen, J, You, Z C. The research and application of magnetic treatment apparatus of tools. *Tool Eng* **29**(10): 22–25 (1995) (in Chinese)

[11] Fu L C, Zhou L P. Effect of applied magnetic field on wear behaviour of martensitic steel. *J Mater Res Technol* **8**(3): 2880–2886 (2019)

[12] Zagoruiko N V. Effect of an electrostatic field and a pulsed magnetic field on movements of dislocations in sodium chloride. *Sov Phys Crystallogr* **10**(1): 63 (1965)

[13] Chebotkevich L A, Urusovskaya A A, Veter V V. Motion of dislocations under the action of a magnetic field. *Kristallografiya* **10**(5): 688–692 (1965)

[14] Hayashi S, Takahashi S, Yamamoto M. Magneto-plastic effect in nickel single crystals. *J Phys Soc Jpn* **30**(2): 381–387 (1971)

[15] Al'shits V I, Darinskaya E V, Perekalina T M. Motion of dislocations in NaCl crystals under the action of a static magnetic field. *Sov Phys Solid State* **29**(2): 265–267 (1987)

[16] Al'shits V I, Darinskaya E V, Petrzhik E A. *In situ* investigation of the magnetoplastic effect in NaCl crystals by the continuous etching method. *Sov Phys Solid State* **33**(10): 1694–1699 (1991)

[17] Alshits V, Darinskaya E, Petrzhik E. Magnetoplastic effect in CsI and LiF crystals. *Phys Solid State* **35**: 162–164 (1993)

[18] Al'Shits V I, Voska R, Darinskaya E V, Petrzhik E A. Magnetoplastic effect in NaCl, LiF, and Al crystals subjected to an alternating magnetic field. *Phys Solid State* **35**(1): 37–39 (1993)

[19] Golovin Y I, Morgunov R B. Effect of a static magnetic field on the mobility of dislocations in NaCl single crystals. *Phys Solid State* **37**(5): 734–739 (1995)

[20] Al'shits V I, Darinskaya E V, Petrzhik E A. Magnetoplastic effect in aluminum single-crystals. *Sov Phys Solid State* **34**(1): 81–83 (1992)

[21] Al'shits V I, Darinskaya E V, Gektina I V, Lavrent'ev F F. Magnetoplastic effect in single crystals of zinc. *Sov Phys Crystallogr* **35**(4): 597–598 (1990)

[22] Alshits V I, Darinskaya E V, Petrzhik E A. Effects of magnetic fields on the dislocation unlocking from paramagnetic centers in non-magnetic crystals. *Mater Sci Eng A* **164**(1–2): 322–326 (1993)

[23] Alshits V I, Darinskaya E V, Kazakova O L, Mikhina E Y, Petrzhik E A. Magnetoplastic effect in nonmagnetic crystals. *Mater Sci Eng A* **234–236**: 617–620 (1997)

[24] Alshits V I, Darinskaya E V, Kazakova O L, Mikhina E Y, Petrzhik E A. Magnetoplastic effect in non-magnetic crystals and internal friction. *J Alloys Compd* **211–212**: 548–553 (1994)

[25] Petrzhik E A, Darinskaya E V, Erofeeva S A, Raukhman M R. Effects of doping and preliminary processing on the magnetically stimulated mobility of dislocations in InSb single crystals. *Phys Solid State* **45**(2): 266–269 (2003)

[26] Darinskaya E V, Petrzhik E A, Erofeev S A, Kisel' V P. Magnetoplastic effect in InSb. *Jetp Lett* **70**(4): 309–313 (1999)

[27] Yugova T G, Belov A G, Knyazev S N. Magnetoplastic effect in Te-doped GaAs single crystals. *Crystallogr Rep* **65**(1): 7–11 (2020)

[28] Zhang X, Cai Z P. Effect of magnetic field on the nanohardness of monocrystalline silicon and its mechanism. *Jetp Lett* **108**(1): 23–29 (2018)

[29] Wu J H, Wray P J, Garcia C I, Hua M J, Deardo A J. Image quality analysis: A new method of characterizing microstructures. *ISIJ Int* **45**(2): 254–262 (2005)

[30] Golovin Y I, Morgunov R B, Zhulikov S E. Effect of a static magnetic field on overcoming short-range obstacles by dislocations in LiF single crystals. *Phys Solid State* **39**(3): 430–431 (1997)

[31] Golovin Y I, Morgunov R B, Ivanov V E. *In situ* investigation of the effect of a magnetic field on the mobility of dislocations in deformed KCl: Ca single crystals. *Phys Solid State* **39**(4): 550–553 (1997)

[32] Golovin Y I, Morgunov R B. Effect of a static magnetic field on the rate of plastic flow of NaCl: Ca single crystals. *Phys Solid State* **37**(7): 1152–1153 (1995)

[33] Golovin Y I, Kazakova O L, Morgunov R B. Mobility of dislocations in NaCl single crystals in a static magnetic field. *Phys Solid State* **35**(5): 700–701 (1993)

[34] Golovin Y I, Morgunov R B. Effect of a weak magnetic field on the state of structural defects and the plasticity of ionic crystals. *J Exp Theor Phys* **88**(2): 332–341 (1999)

[35] Wu S, Lu A, Zhao H, Fang H, Tang F. Micromechanism of residual stress reduction by low frequency alternating magnetic field treatment. *Mater Sci Eng A* **328**(1–2): 133–136 (2002)

[36] Huang X Q. Research on improving bearing life by pulsed magnetic treatment. Ph.D. Thesis. Beijing (China): Tsinghua University, 2011

[37] Cai Z P, Lin J A, Zhou L A, Zhao H Y. Evaluation of effect of magnetostriction on residual stress relief by pulsed magnetic treatment. *Mater Sci Technol* **20**(12): 1563–1566 (2004)

[38] Nabarro F N. Dislocations in a simple cubic lattice. *Proc Phys Soc* **59**(2): 256–272 (1947)

[39] Akram S, Babutskyi A, Chrysanthou A, Montalvão D, Pizúrová N. (2019) Effect of alternating magnetic field on the fatigue behaviour of EN_8 steel and 2014-T6 aluminium alloy. *Metals* **9**(9): 984 **(**2019)

[40] Xu Q D, Li K J, Cai Z P, Wu Y. Effect of pulsed magnetic field on the microstructure of TC4 titanium alloy and its mechanism. *Acta Metall Sin* **55**(4): 489–495 (2019)

[41] Vespucci S, Winkelmann A, Naresh-Kumar G, Mingard K P, Maneuski D, Edwards P R, Day A P, O'Shea V, Trager-Cowan C. Digital direct electron imaging of energy-filtered electron backscatter diffraction patterns. *Phys Rev B* **92**(20): 205301 (2015)

[42] Zhang X, Zhao Q A, Cai Z P, Pan J L. Effects of magnetic field on the residual stress and structural defects of Ti-6Al-4V. *Metals* **10**(1): 141 (2020)

[43] Qian C K, Li K J, Rui S S, Hou M, Zhang X, Wu Y, Cai Z P. Magnetic induced re-dissolution and microstructure modifications on mechanical properties of Cr_4Mo_4V steel subjected to pulsed magnetic treatment. *J Alloys Compd* **881**: 160471 (2021)

[44] Jin Y, Chao Y S, Liu F, Wang J G, Sun M T. Nanocrystallization and magnetostriction coefficient of $Fe_{52}Co_{34}Hf_7B_6Cu_1$ amorphous alloy treated by medium-frequency magnetic pulse. *J Magn Magn Mater* **468**: 181–184 (2018)

[45] Chao Y S, Zhang Y H, Guo H, Zhang L, Wang X G. Low temperature nano crystallization of Fe78Si9B13 amorphous alloy treated by low-frequency magnetic pulsing. *Acta Metall Sin* **43**(3): 231–234 (2007)

[46] Qian C K, Liu Q, Xiong X Y, Ye B J, Li Z Y, Li K J, Ying S J, Zhang H J, Huang D M, Zhang X, *et al*. Mechanism for magnetic field induced structural relaxation and accompanying fracture toughness improvement of the thermal spraying coating. *Mater Des* **223**: 111113 (2022)

[47] Balluffi R W, Brokman A, King A H. CSL/DSC Lattice model for general crystalcrystal boundaries and their line defects. *Acta Metall* **30**(8): 1453–1470 (1982)

[48] Hou M D. Research of magnetic field treatment on the partial mechanical properties of M50 bearing steel. Master Thesis. Beijing (China): Tsinghua University, 2020

[49] Csanádi T, Vojtko M, Dusza J. Deformation and fracture of WC grains and grain boundaries in a WC-Co hardmetal during microcantilever bending tests. *Int J Refract Met Hard Mater* **87**: 105163 (2020)

[50] Shao Q A, Kang J J, Xing Z G, Wang H D, Huang Y F, Ma G Z, Liu H P. Effect of pulsed magnetic field treatment on the residual stress of $20Cr_2Ni4A$ steel. *J Magn Magn Mater* **476**: 218–224 (2019)

[51] Shao Q. Effect of pulsed magnetic field treatment on mechanical properties and fatigue life of 20Cr2Ni4A steel. Master Thesis. Beijing (China): China University of Geosciences, 2019

[52] Li G R, Li Y M, Wang F F, Wang H M. Microstructure and performance of solid TC4 titanium alloy subjected to the high pulsed magnetic field treatment. *J Alloys Compd* **644**: 750–756 (2015)

[53] Hou M D, Li K J, Li X G, Zhang X, Rui S S, Wu Y, Cai Z P. Effects of pulsed magnetic fields of different intensities

on dislocation density, residual stress, and hardness of Cr_4Mo_4V steel. *Crystals* **10**(2): 115 (2020)

[54] Yan M, Wang C, Luo T J, Li Y J, Feng X H, Huang Q Y, Yang Y S. Effect of pulsed magnetic field on the residual stress of rolled magnium alloy AZ31 sheet. *Acta Metall Sin Engl Lett* **34**(1): 45–53 (2021)

[55] Wang, H M, Peng, C X, Li, G R, Li, P S. Mechanism of high magnetic field on aluminum matrix composites dislocation density. *J Cent South Univ Sci Technol* **48**(2): 325–330 (2017) (in Chinese)

[56] Buchachenko A L. Effect of magnetic field on mechanics of nonmagnetic crystals: The nature of magnetoplasticity. *J Exp Theor Phys* **102**(5): 795–798 (2006)

[57] Badylevich M V, Kveder V V, Orlov V I, Ossipyan Y A. Spin-resonant change of unlocking stress for dislocations in silicon. *Phys Stat Sol* (*C*) **2**(6): 1869–1872 (2005)

[58] Golovin Y I. Magnetoplastic effects in crystals in the context of spin-dependent chemical kinetics. *Crystallogr Rep* **49**(4): 668–675 (2004)

[59] Alshits V I, Darinskaya E V, Koldaeva M V, Petrzhik E A. Magnetoplastic effect: Basic properties and physical mechanisms. *Crystallogr Rep* **48**(5): 768–795 (2003)

[60] Morgunov R B, Buchachenko A L. Magnetic field response of NaCl: Eu crystal plasticity due to spin-dependent Eu^{2+} aggregation. *Phys Rev B* **82**: 014115 (2010)

[61] Morgunov R B, Buchachenko A L. Magnetoplasticity and magnetic memory in diamagnetic solids. *J Exp Theor Phys* **109**(3): 434–441 (2009)

[62] Alshits V I, Darinskaya E V, Koldaeva M V, Petrzhik E A. Magnetoplastic effect in nonmagnetic crystals. In *Dislocations in Solids*. Hirth J P, Ed. Amsterdam: Elsevier, 2008: 333–438

[63] Molotskii M, Fleurov V. Spin effects in plasticity. *Phys Rev Lett* **78**(14): 2779–2782 (1997)

[64] Brocklehurst B. Formation of excited states by recombining organic ions. *Nature* **221**(5184): 921–923 (1969)

[65] Turro N J. Influence of nuclear spin on chemical reactions: Magnetic isotope and magnetic field effects (a Review). *Proc Natl Acad Sci U S A* **80**(2): 609–621 (1983)

[66] Turro N J. Micelles, magnets and molecular mechanisms. Application to cage effects and isotope separation. *Pure Appl Chem* **53**(1): 259–286 (1981)

[67] Alshits V I, Darinskaya E V, Kazakova O L, Mikhina E Y, Petrzhik E A. Magnetoplastic effect and spin-lattice relaxation in a dislocation-paramagnetic-center system. *Jetp Lett* **63**(8): 668–673 (1996)

[68] Al'shits V I, Darinskaya E V. Magnetoplastic effect in LiF crystals and longitudinal spin relaxation. *Jetp Lett* **70**(11): 761–766 (1999)

[69] Zhang X, Zhao Q A, Wang Z Y, Cai Z P, Pan J L. A study on the room-temperature magnetoplastic effect of silicon and its mechanism. *J Phys*: *Condens Matter* **33**(43): 435702 (2021)

[70] Dai N. Investigation and application of microwave-magnetic field strengthening mechanism of CBN cutting tools based on ESR effect. Master Thesis. Beijing (China): Tsinghua University, 2022

[71] Song Y L, Yu C, Yu H L, Zhao C Y. Mechanical properties improvement of laser tailor welded blanks of DP600 steel by magnetic treatment. *Metals* **7**(3): 85 (2017)

[72] Zhang X. Effects of magnetic field on microstructure and mechanical properties of titanium alloy TC4 and the action mechanism. Ph.D. Thesis. Beijing (China): Tsinghua University, 2022

[73] Song Y L, Yu C, Miao X, Han X H, Qian D S, Chen X. Tribological performance improvement of bearing steel GCr15 by an alternating magnetic treatment. *Acta Metall Sin Engl Lett* **30**(10): 957–964 (2017)

[74] Skvortsov A A, Pshonkin D E, Luk'yanov M N, Rybakova M R. Influence of permanent magnetic fields on creep and microhardness of iron-containing aluminum alloy. *J Mater Res Technol* **8**(3): 2481–2485 (2019)

[75] Wang X Z, Zhang X, Liu Q, Qian C K, Cai Z P. Enhanced low cycle fatigue properties of Ti-6Al-4V alloy by post-treatment technology of pulse high-intensity magnetic field. *J Mater Eng Perform* **32**(22): 10029–10038 (2023)

[76] Galustashvili M V, Driaev D G, Kvatchadze V G. Magnetoplastic effect under stress relaxation in NaCl crystals. *Jetp Lett* **110**(12): 785–788 (2019)

[77] Urusovskaya A A, Al'shits V I, Smirnov A E, Bekkauer N N. On the effect of a magnetic field on the yield point and kinetics of macroplasticity in LiF crystals. *Jetp Lett* **65**(6): 497–501 (1997)

[78] Al'shits V I, Urusovskaya A A, Smirnov A E, Bekkauer N N. Deformation of LiF crystals in DC magnetic field. *Phys Solid State* **42**(2): 277–279 (2000)

[79] Al'shits V I, Bekkauer N N, Smirnov A E, Urusovskaya A A. Effect of a magnetic field on the yield point of NaCl crystals. *J Exp Theor Phys* **88**(3): 523–526 (1999)

[80] Badylevich M V, Iunin Y L, Kveder V V, Orlov V I, Osipyan Y A. Influence of magnetic field on critical stress and mobility of dislocations in silicon. *Solid State Phenom* **95-96**: 433–437 (2004)

[81] Ossipyan Y A, Morgunov R B, Baskakov A A, Orlov A M, Skvortsov A A, Inkina E N, Tanimoto Y. Magnetoresonant hardening of silicon single crystals. *Jetp Lett* **79**(3): 126–130 (2004)

[82] Liu T, Liu M S. Molecular simulation of the relationship between elastic constants of metals and temperature. *Mater Mech Eng* **38**(4): 73–77, 81 (2014) (in Chinese)

[83] Liu T, Liu M S. Theoretical analysis of the relationship between elastic constants of metals and temperatures. *Mater Mech Eng* **38**(3): 85–89, 95(2014) (in Chinese)

[84] Atzori B, Lazzarin P. Notch sensitivity and defect sensitivity under fatigue loading: Two sides of the same medal. *Int J Fract* **107**(1): L3–L8 (2001)

[85] Sangid M D, Ezaz T, Sehitoglu H, Robertson I M. Energy of slip transmission and nucleation at grain boundaries. *Acta Mater* **59**(1): 283–296 (2011)

[86] Wright W J, Schwarz R B, Nix W D. Localized heating during serrated plastic flow in bulk metallic glasses. *Mater Sci Eng A* **319–321**: 229–232 (2001)

[87] Smith S, Melkote S N, Lara-Curzio E, Watkins T R, Allard L, Riester L. Effect of surface integrity of hard turned AISI 52100 steel on fatigue performance. *Mater Sci Eng A* **459**(1–2): 337–346 (2007)

[88] Guan J, Wang L Q, Zhang Z Q, Shi X J, Ma X X. Fatigue crack nucleation and propagation at clustered metallic carbides in M50 bearing steel. *Tribol Int* **119**: 165–174 (2018)

[89] Jelita Rydel J, Toda-Caraballo I, Guetard G, Rivera-Díaz-del-Castillo P E J. Understanding the factors controlling rolling contact fatigue damage in VIM-VAR M50 steel. *Int J Fatigue* **108**: 68–78 (2018)

[90] Zhao Y C, Zhang Z L, Yan C G, Li M L. The effect of magnetization treating on the contact fatigue characteristic of GCr15 steel. *Mater Mech Eng* **29**(3): 50–51 (2005) (in Chinese)

[91] Vanderwert T. Magnetic process relieves stress in cutting tools. *Cutt Tool Eng* **39**(5): 45-46, 49 (1987)

[92] Klamecki B E. Residual stress reduction by pulsed magnetic treatment. *J Mater Process Technol* **141**(3): 385–394 (2003)

[93] Lu A L, Tang F, Luo X J, Mei J F, Fang H Z. Research on residual-stress reduction by strong pulsed magnetic treatment. *J Mater Process Technol* **74**(1–3): 259–262 (1998)

[94] Tang F, Lu A L, Mei J F, Fang H Z, Luo X J. Research on residual stress reduction by a low frequency alternating magnetic field. *J Mater Process Technol* **74**(1–3): 255–258 (1998)

[95] Cai Z P, Lin J A, Zhao H Y, Lu A L. Orientation effects in pulsed magnetic field treatment. *Mater Sci Eng A* **398**(1–2): 344–348 (2005)

[96] Lin J. Study on reduction of residual stress in steel materials by pulsed magnetic treatment. Ph.D. Thesis. Beijing (China): Tsinghua University, 2006

[97] Cai Z P, Duan X J, Lin J, Zhao H Y. Magnetostriction varieties and stress relief caused by pulsed magnetic field. *Front Mech Eng* **6**(3): 354–358 (2011)

[98] Song Y L, Hua L, Wang B. Reduction of residual stress in low alloy steel with magnetic treatment in different directions. *J Wuhan Univ Technol Mater Sci Ed* **24**(6): 857–862 (2009)

[99] Song Y L, Hua L. Mechanism of residual stress reduction in low alloy steel by a low frequency alternating magnetic treatment. *J Mater Sci Technol* **28**(9): 803–808 (2012)

[100] Bouzakis K-D, Michailidis N, Skordaris G, Bouzakis E, Biermann D, M'Saoubi R. Cutting with coated tools: Coating technologies, characterization methods and performance optimization. *CIRP Annals* **61**(2): 703–723 (2012)

[101] Xu Q. Research and application on magnetoplasticity effect of coated cemented carbide cutting tools. Master Thesis. Beijing (China): Tsinghua University, 2019

[102] Fei H L, Wu H Y, Yang X D, Xiong J, Zhang L, Chen Z, Jiang K, Liu J. Pulsed magnetic field treatment of cBN tools for improved cutting performances. *J Manuf Process* **69**: 21–32 (2021)

[103] Hou M D, Mou W P, Yan G H, Song G, Wu Y, Ji W, Jiang Z X, Wang W, Qian C K, Cai Z P. Effects of different distribution of residual stresses in the depth direction on cutting performance of TiAlN coated WC-10wt%Co tools in milling Ti-6Al-4V. *Surf Coat Technol* **397**: 125972 (2020)

[104] Ahmed R, Yu H, Stoica V, Edwards L, Santisteban J R. Neutron diffraction residual strain measurements in post-treated thermal spray cermet coatings. *Mater Sci Eng A* **498**(1–2): 191–202 (2008)

[105] Qian C K, Liu Q, Wang H, Li K J, Cai Z P. Interface strengthening for thermal sprayed WC-10Co4Cr coating subjected to pulsed magnetic treatment. *Rare Metals* **43**(2): 780–795 (2024)

[106] Lopez E, Beltzung F, Zambelli G. Measurement of cohesion and adhesion strengths in alumina coatings produced by plasma spraying. *J Mater Sci Lett* **8**(3): 346–348 (1989)

[107] Abdoos M, Bose B, Rawal S, Arif A F M, Veldhuis S C. The influence of residual stress on the properties and performance of thick TiAlN multilayer coating during dry turning of compacted graphite iron. *Wear* **454–455**: 203342 (2020)

[108] Fu H, He Y Y, Yang J, Fu Y H, Yin B F, Zhang Y H, Ji J H, Gu Z H, Zhou Y. Enhancing adhesion strength of PVD AlCrN coating by novel volcano-shaped micro-textures: Experimental study and mechanism insight. *Surf Coat Technol* **445**: 128712 (2022)

[109] Forster N H, Rosado L, Ogden W P, Trivedi H K. Rolling contact fatigue life and spall propagation characteristics of AISI M50, M50 NiL, and AISI 52100, part III: Metallurgical examination. *Tribol Trans* **53**(1): 52–59 (2009)

[110] El Laithy M, Wang L, Harvey T J, Vierneusel B, Correns M, Blass T. Further understanding of rolling contact fatigue in rolling element bearings—A review. *Tribol Int* **140**: 105849 (2019)

[111] Warhadpande A, Sadeghi F, Evans R D. Microstructural alterations in bearing steels under rolling contact fatigue part 1—Historical overview. *Tribol Trans* **56**(3): 349–358 (2013)

[112] Chen Y H, Wang J, Chen M. Enhancing the machining performance by cutting tool surface modifications: A focused review. *Mach Sci Technol* **23**(3): 477–509 (2019)

[113] Bataineh O, Klamecki B, Koepke B G. Effect of pulsed magnetic treatment on drill wear. *J Mater Process Technol* **134**(2): 190–196 (2003)

[114] Yang Y F, Yang Y, Liao C Z, Yang G, Qin Y, Li Q Q, Wu M X. Enhancing tribological performance of cemented carbide (WC-^{12}Co) by pulsed magnetic field treatment and magnetofluid. *Tribol Int* **161**: 107086 (2021)

[115] Yang Y F, Yang Y, Li Q Q, Qin Y, Yang G, Zhou B H, Deng C J, Wu M X. An eco-friendly pulsed magnetic field treatment on cemented carbide (WC–^{12}Co) for enhanced milling performance. *J Clean Prod* **340**: 130748 (2022)

[116] Liu J, Wei C, Yang G, Wang L B, Wang L, Wu X L, Jiang K, Yang Y. A novel combined electromagnetic treatment on cemented carbides for improved milling and mechanical performances. *Metall Mater Trans A* **49**(10): 4798–4808 (2018)

[117] Li Q Q, Yang Y, Yang Y F, Li P Y, Yang G, Liu J, Wu M X. Enhancing the wear performance of WC-6Co tool by pulsed magnetic field in Ti-6Al-4V machining. *J Manuf Process* **80**: 898–908 (2022)

[118] Zhang L, Chen Z, Wen H T, Wu M X, Yang Y, Jiang K, Liu J. Modification effects of the pulsed magnetic field on the coated cemented carbides tool for enhanced mechanical and cutting performances. *Int J Refract Met Hard Mater* **111**: 106093 (2023)

[119] Liu J C, Yamazaki K, Ueda H, Narutaki N, Yamane Y. Machinability of pearlitic cast iron with cubic boron nitride (CBN) cutting tools. *J Manuf Sci Eng* **124**(4): 820–832 (2002)

[120] Chou Y S. Wear mechanisms of cubic boron nitride tools in precision turning of hardened steels. Ph.D. Thesis. Ann Arbor (United States): Purdue University, 1994

[121] Li G R, Qin T, Fei A G, Wang H M, Zhao Y T, Chen G, Kai X Z. Performance and microstructure of TC4 titanium alloy subjected to deep cryogenic treatment and magnetic field. *J Alloys Compd* **802**: 50–69 (2019)

[122] Li Z, Li K J, Qian C K, Wang D X, Ji W, Wu Y, Cai Z P, Liu Q. Effect of pulsed magnetic field on retained austenite of quenched $8Cr_4Mo_4V$ steel under cryogenic condition. *J Mater Res Technol* **23**: 5004–5015 (2023)

[123] He G Z, Qian C K, Cai Z P, Li K J, Liu Q, Yan J F. Magnetic field-assisted laser shock peening of Ti_6Al_4V alloy. *Adv Eng Mater* **25**(10): 2201843 (2023)

Zhipeng CAI. He received his M.S. and Ph.D. degrees in mechanical engineering from Tsinghua University in 1999 and 2001, respectively. He joined the Department of Mechanical Engineering at Tsinghua University from 2002. His current position is a research fellow. His research area covers the microstructure characterization and regulation of welded joints and the application of pulsed magnetic treatment.